

Methods and aspects of active-RC filter synthesis

Citation for published version (APA):

Bokhoven, van, W. M. G. (1970). *Methods and aspects of active-RC filter synthesis*. (EUT report. E, Fac. of Electrical Engineering; Vol. 71-E-27). Technische Universiteit Eindhoven.

Document status and date:

Published: 01/01/1970

Document Version:

Publisher's PDF, also known as Version of Record (includes final page, issue and volume numbers)

Please check the document version of this publication:

- A submitted manuscript is the version of the article upon submission and before peer-review. There can be important differences between the submitted version and the official published version of record. People interested in the research are advised to contact the author for the final version of the publication, or visit the DOI to the publisher's website.
- The final author version and the galley proof are versions of the publication after peer review.
- The final published version features the final layout of the paper including the volume, issue and page numbers.

[Link to publication](#)

General rights

Copyright and moral rights for the publications made accessible in the public portal are retained by the authors and/or other copyright owners and it is a condition of accessing publications that users recognise and abide by the legal requirements associated with these rights.

- Users may download and print one copy of any publication from the public portal for the purpose of private study or research.
- You may not further distribute the material or use it for any profit-making activity or commercial gain
- You may freely distribute the URL identifying the publication in the public portal.

If the publication is distributed under the terms of Article 25fa of the Dutch Copyright Act, indicated by the "Taverne" license above, please follow below link for the End User Agreement:

www.tue.nl/taverne

Take down policy

If you believe that this document breaches copyright please contact us at:

openaccess@tue.nl

providing details and we will investigate your claim.

METHODS AND ASPECTS
OF ACTIVE - RC FILTER SYNTHESIS

by

W.M.G. van Bokhoven

Eindhoven University of Technology
Eindhoven The Netherlands;
Department of Electrical Engineering.

METHODS AND ASPECTS OF ACTIVE - RC FILTER SYNTHESIS

by

W.M.G. van Bokhoven.

T.H.-report 71-E-27

ISBN 90 6144 027 0

10 December 1970.

Submitted in partial fulfillment of the requirements for the
degree of Ir. (M.Sc.) at the Eindhoven University of Technology,
Department of Electrical Engineering.

C O N T E N T S

INTRODUCTION	page 1
Ch. 1.1 <u>Approximation.</u>	3
1.2 General low-pass filter approximation.	3
1.2.1 Butterworth approximation.	5
1.2.2 Chebychev approximation.	6
1.2.3 Elliptic approximation.	7
1.3.1 General properties of the elliptic transferfunction modulus.	8
1.3.2 Algebraic derivation of second and fourth degree elliptic transferfunction modulus.	12
Ch. 2.1 <u>Network sensitivity.</u>	20
2.2.1 Sensitivity functions for second order low-pass LCR-filters.	21
2.2.2 Sensitivity calculation for an active low-pass filter.	24
2.2.3 Sensitivities for the Fjälbrant filter.	25
Ch. 3.1 <u>Active filters obtained by substitution methods.</u>	27
3.2.1 Gyrator-capacitor substitution.	27
3.2.2 Gyrator circuits.	28
3.3 Active synthesis using frequency dependent negative resistors.	33
Ch. 4 <u>Active filters on synthesis basis.</u>	38
4.1 Negative Impedance Convertor synthesis.	38
4.1.1 Sensitivity considerations for the Linvill-synthesis.	41
4.2 Synthesis method of Yaganisawa.	43
4.3 Synthesis with the gyrator as a two-port.	45
4.3.1 Sensitivities for the RC gyrator two-port synthesis.	48

4.4	Synthesis with PICs by the Antoniou method.	49
4.4.1	Special cases for the Antoniou method.	51
Ch. 5	<u>Cascade synthesis with second order sections.</u>	54
5.1	Second and third order low-pass Fjälbrant filters.	54
5.2	Active realizations of second order Notch filters with a modified Twin-T network.	56
5.3	Active filters employing negative feedback.	57
5.4	Second order filters with PICs.	60
Appendix.		61
References.		68

INTRODUCTION.

In many fields of electrical engineering filters are used to perform or equalise amplitude, phase as well as delay characteristics. The circuits becoming more and more complex with the refined application of electronics nowadays, need for microminiaturisation in order to limit the physical size to a reasonable one.

In the last ten years great progress was made in miniaturising resistors and capacitors as well as active elements however inductances still kept their same size because a certain volume is needed to store the magnetic energy connected with the value of the self inductance and the current flowing through it. Only magnetic materials with a higher permeability would improve the quotient inductance-volume and with the state of the art of ferromagnetic materials at this time no revolutionary progress has to be expected.

On the other hand the tendency is growing in realizing complete circuits in monolithic form on one chip of semiconductor material, filters included, to get better stability and reliability at the same time.

Since classical filter synthesis leads to the use of inductances together with capacitors and resistors, it's impossible to design integrated filters with this method, unless the inductances are simulated in one or other way.

This simulation can be done by means of gyrators which method has the advantage that one can use known synthesis methods and merely replaces the inductors by gyrators terminated with capacitors. From synthesis point of view there will be no trouble, however a lot of active components are needed so that the circuit in general

won't be an economical one and the simulation of floating inductors demands for an even higher complexity.

As a second possibility the gyrator, being passive however mostly build up with active elements, can be used as element in a new synthesis method based on R-C networks coupled with the gyrator considered as a two-port network, trying to make full use of its property's and thus in a certain way minimising the number of implicit active elements. Also negative impedance convertors and various other active elements can be used to realise filter networks on a synthesis basis each having its own advantages, limitations and disadvantages.

The third method consists in fact in splitting up the filter transferfunction in first and second order parts, each of wich can be realized by a suitable active circuit together with R-C elements.

Because of the great number of active second order filter realisations a wide variety of circuits is possible and one has to use extra design criteria, not always being electrical ones, to make the best choice.

The intention of this paper is to describe and compare some lumped R-C active filter realisations and synthesis methods of the above three groups on a basis of sensitivity and stability, wich appears to be usefull criteria for practical utilisation of the designed filters.

As apparent from the foregoing for show^{rt}ness sake no attempt has been made to investigate the wide class of digital and switched filters, although these methods become more and more promising in the near future.

1. Approximation.

1.1. Electric filters are used to realize prescribed input-output relations for the signal passing through. These relations may be given in terms of amplitude or phase response of the given signal or otherwise be specified. Generally these specifications are given as a tolerance field in amplitude and phase frequency characteristics while mostly only one of them will be prescribed and the other one is concerned to be of no importance. The filter to be designed has to meet these specifications i.e. must lead to a response full filling the tolerance conditions being set. Thus the filter design starts with the determination of the transferfunction from the prescribed limitations where after this transferfunction must be synthesized. In order to present a more closed description of the synthesis methods some of these approximations will be treated in the next chapters, mainly following ref. (1) in notation and derivation.

1.2. The general low-pass filter approximation.

An important class of filters is formed by the so called low-pass filters, which approximate the modulus of a transferfunction in such a way that signals with their frequency ranging from zero to the frequency f_0 will be passed without much attenuation while signals with frequency exceeding f_a will be strongly attenuated. The tolerance field for this type of filters has the general form of fig.1. Here in the frequency axis is divided in three main parts, obviously characterized as:

part I - passband

part II - transition band

part III - attenuation band or stopband

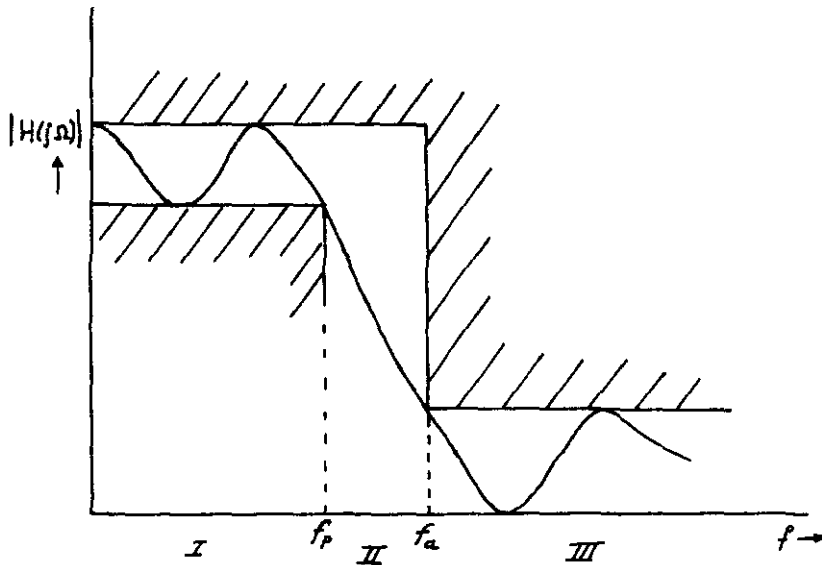


fig.1.

Constructing a transferfunction from a given tolerance field is accomplished by derivation of the modulus as a pure mathematical approximation of this tolerance field with an even function of the radiant frequency. Here after the transferfunction itself is obtained from the constructed modulus on a basis of network theoretical prescriptions.

The above mentioned approximation can proceed as follows.

Let the modulus to be approximated be the modulus of a voltage transferfunction $H(p)$ defined by

$$\frac{V_{out}}{V_{in}} = H(p) \text{ and } p = j\Omega, \text{ where in } V_{in} \text{ and } V_{out}$$

are the amplitudes of the sinusoidal steady-state excitation and response.

The squared modulus of the lowpass filter can be written in the general normalised form as

$$|H(j\Omega)|^2 = \frac{1}{1 + H^2 \Phi^2(\Omega)} \quad (1)$$

Here in $\Phi(\Omega)$ is an even or odd function in Ω called the characteristic function and H is a constant.

Defining the transfer loss α as

$$\alpha = -20 \log \frac{[V_{out}]}{|H(j\Omega)|} \text{ dB}$$

this leads to

$$\alpha = 10 \log [1 + H^2 \Phi^2(\Omega)] \quad \text{dB} \quad (2)$$

In this notation the modulus indeed is characterized by the choice of the characteristic function.

1.2.1 Butterworth approximation.

Taking $\Phi(\Omega) = \Omega^n$ (3)

leads to the Butterworth or maximally flat approximation based on the property that in the point $\Omega = 0$ the first $2n-1$ derivatives of the denominator of (1) become zero, resulting in a flat pass of the curve near $\Omega = 0$. Furthermore the denominator increases monotonically with Ω leading to a monotonic fall-off for the modulus itself. For the Butterworth type from (2) and (3) this results in an asymptotic increase in transfer loss with $6n$ dB per octave for $H\Omega^n \gg 1$. In fig.2 some of these curves are drawn normalized for equal Ω_c , being the frequency where α is 3 dB down.

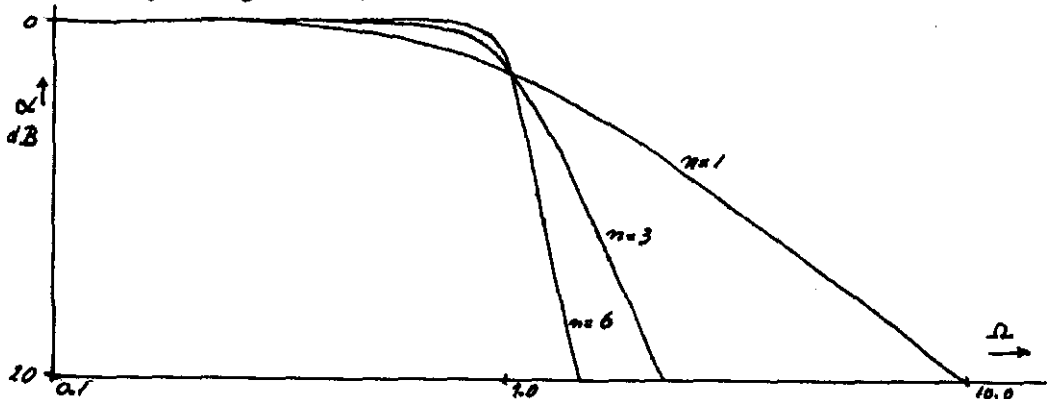


fig. 2. Normalized Butterworth low-pass transfer-loss.

For this type of approximation there will be no difficulty in selecting n and H that way, that the resulting loss characteristic is lying in the given tolerance field.

For a rapid fall off in the stopband however a large n is needed leading to an excessive number of filter elements as compared with the Chebychev approximation given in the following chapter.

1.2.2 Chebychev approximation.

By taking $\mathbb{B}(\Omega) = T_n(\Omega)$

with $T_n(\Omega) = \cos [n \arccos \Omega]$ for $\Omega \leq 1$ (see fig.3)

a Chebychev approximation is obtained. $T_n(\Omega)$ can also be written as

$$T_n(\Omega) = \frac{n}{2} \sum_{m=0}^{\lfloor \frac{n}{2} \rfloor} (-1)^m \frac{(n-m-1)!}{m! (n-2m)!} (2\Omega)^{n-2m} \quad (\text{see ref [2]})$$

The passband ranging from $\Omega = 0$ to $\Omega = 1$ shows $n/2$ equal amplitude ripples between a minimum and a maximum value determined by the constant H .

In the transition and stopband ($\Omega > 1$) $|T_n(\Omega)|$ increases monotonically with Ω again producing an asymptotic increase in transfer loss of $6n$ dB per octave. In comparison with the Butterworth approximation the value of n can be taken smaller for the same tolerance field leading to fewer elements in the final realisation.

Some Chebychev characteristics are given in fig. 4.

Because the extrema of $T_n(\Omega)$ in the passband all have modulus 1 the ripple amplitude is determined by

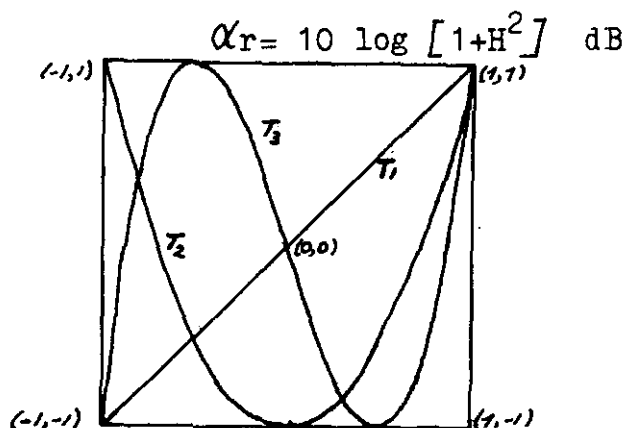


fig.3 Chebychev function $T_n(\Omega)$

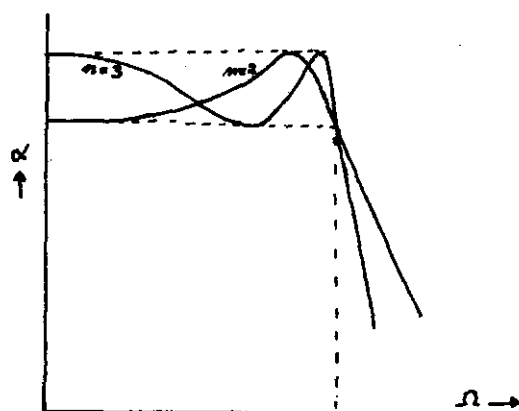


fig.4 Chebychev low-pass transfer-loss

1.2.3 Elliptic approximation.

As stated in 1.2.2 introducing a ripple in the pass-band leads to fewer elements in the final realization. As a consequence this suggests an approximation having also ripples in the stop-band, probably will reduce further the number of elements as compared with the previous chebychev type.

Specially if the number of stopband ripples is taken to be equal to the number of passband ripples a so called elliptic approximation is obtained if $\mathcal{D}(a)$ satisfies certain relations expressable in Jacobi elliptic functions.

This type of approximation leads to points of infinite attenuation in the stopband, together with a fast fall-off in the transitionband.

Because the relative few number of elements needed to approximate a certain attenuation this filter type is an interesting one for application in active filter design where, as we'll see later on, the sensitivity plays an important role and the more complex a network is, the more difficult it will be to realise the filter with the required accuracy and stability.

Unfortunately however the calculation of the transfer-function for a given tolerance field is much more difficult for this filter type as compared with the previous ones but the gain in simplicity for the final network makes the effort worthwhile. On the other hand it appears to be easy to calculate the transferfunction in an algebraic way if the degree of the filter is small (up to 4).

Therefore in the following the algebraic method is explained first and ^{in an appendix} ~~later~~ on the formulas will be given for the calculation of the higher order filters.

1.3.1 General properties of the elliptic transferfunction modulus.

Consider the given tolerance field of fig. 5.

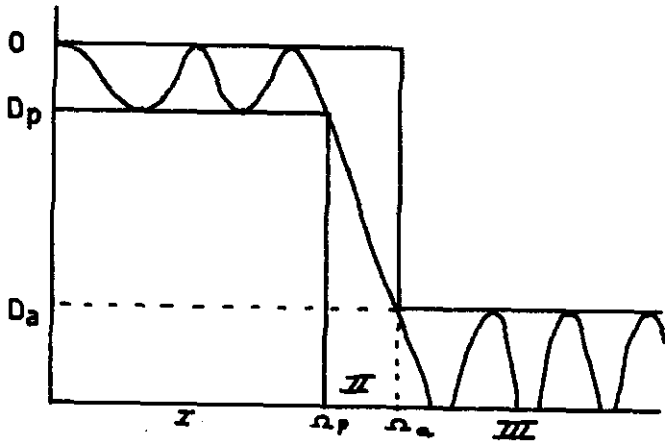


fig. 5.

Here in a maximum loss of D_p dB in the passband ($\Omega < \Omega_p$) and a minimum loss of D_a dB in the stopband ($\Omega > \Omega_a$) are prescribed.

Let the curve of fig. 5 lying in the tolerance field have ν ripples in pass- and stopband. The number of transitions between the two extrema in the passband is given by n , so

$$\nu = \left[\frac{n}{2} \right]$$

The frequencies where the modulus becomes extremal will be denoted as in fig. 6.

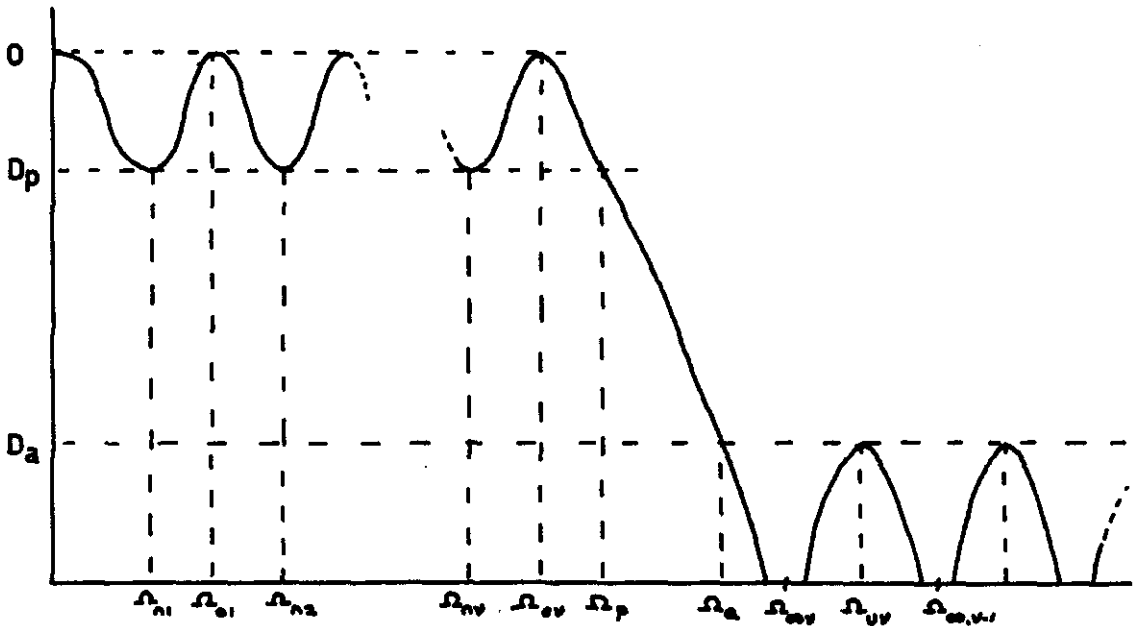


fig. 6.

Let therefore the frequency be normalized such that

$$\Omega_p \Omega_a = 1 \quad (3)$$

and
$$\Phi(\Omega) = \frac{1}{\Phi(\frac{1}{\Omega})} \quad (4)$$

Equation (4) relates the value of $\Phi(\Omega)$ in the band $\Omega \leq 1$ to its value for $\Omega' = \frac{1}{\Omega} \geq 1$ in a reciprocal way. This implies that an equiripple behaviour for $\Omega \leq 1$ also gives equiripple behaviour for $\Omega \geq 1$.

Furthermore for frequencys Ω_{os} lying in the passband

$$0 \leq \Omega \leq \Omega_p < 1 \quad \text{we have}$$

$$\Phi(\Omega_{os}) = 0 \quad s = 1, 2, \dots, \nu.$$

as a consequence of (4) this results in

$$\Phi(\frac{1}{\Omega_{os}}) = \infty$$

and thus (4) implies
$$\Omega_{os} = \frac{1}{\Omega_{os}} \quad (5)$$

Also a maximum value of $\Phi(\Omega)$ in the passband will lead to a minimum value of $\Phi(\Omega)$ in the stopband related by

$$\Phi(\Omega_{ns}) = \pm L = \frac{1}{\Phi(\Omega_{us})} = \pm \frac{1}{K} \quad (6)$$

and
$$\Omega_{us} = \frac{1}{\Omega_{ns}} \quad (7)$$

As a consequence of (3) also
$$\Omega_a = \frac{1}{\Omega_p} \quad , \quad (8)$$

relating the bandedge frequencys in a reciprocal way too. From (6) follows $K = \frac{1}{L}$ expressing the stopband ripple of $\Phi(\Omega)$ in its passband one.

The above points out that relation (4) indeed connects the

stopband in a one to one correspondence with the passband satisfying all the necessary conditions.

Taking $\Phi(\Omega) = \prod_i \frac{f_i(\Omega)}{g_i(\Omega)}$ together with (4) leads to

$$\prod_i \frac{f_i(\Omega)}{g_i(\Omega)} = \prod_i \frac{g_i(\frac{1}{\Omega})}{f_i(\frac{1}{\Omega})}$$

This relation can be satisfied if $g_i(\Omega) = f_i(\frac{1}{\Omega})$ leading to

$$\Phi(\Omega) = \prod_i \frac{f_i(\Omega)}{f_i(\frac{1}{\Omega})}$$

Because $\Phi(\Omega)$ must become zero for $\Omega = \Omega_{oi}$, a reasonable choice for $f_i(\Omega)$ will be

$$f_i(\Omega) = \Omega^2 - \Omega_{oi}^2, \quad i = 1, 2, \dots, v. \quad \text{resulting in}$$

$$\Phi(\Omega) = \prod_i \frac{\Omega^2 - \Omega_{oi}^2}{\frac{1}{\Omega^2} - \Omega_{oi}^2} \quad (9)$$

As Ω^m also satisfies equation (4) we can transform (9) into

$$\left. \begin{aligned} \Phi(\Omega) &= \prod_i \frac{\Omega^2 - \Omega_{oi}^2}{\Omega^2 \Omega_{oi}^2 - 1} && \text{for even } \Phi(\Omega) \\ \Phi(\Omega) &= \Omega \prod_i \frac{\Omega^2 - \Omega_{oi}^2}{\Omega^2 \Omega_{oi}^2 - 1} && \text{for odd } \Phi(\Omega) \end{aligned} \right\} \quad (10)$$

From (2) and (6) the value of L and H can be calculated giving

$$D_p = 10 \log(1 + H^2 L^2)$$

$$D_a = 10 \log(1 + H^2 / L^2)$$

which leads to
$$\left. \begin{aligned} H^4 &= (10^{0.1 D_p} - 1)(10^{0.1 D_a} - 1) \\ L^4 &= (10^{0.1 D_p} - 1) / (10^{0.1 D_a} - 1) \end{aligned} \right\}$$

(11)

1.3.2 Algebraic derivation of second and fourth degree elliptic transferfunction modulus.

For second degree $\mathcal{D}(\Omega)$ equation (10) leads to

$$\mathcal{D}(\Omega) = \frac{\Omega^2 - \Omega_{01}^2}{\Omega^2 \Omega_{01}^2 - 1} \quad (12)$$

This function is shown in fig. 8.

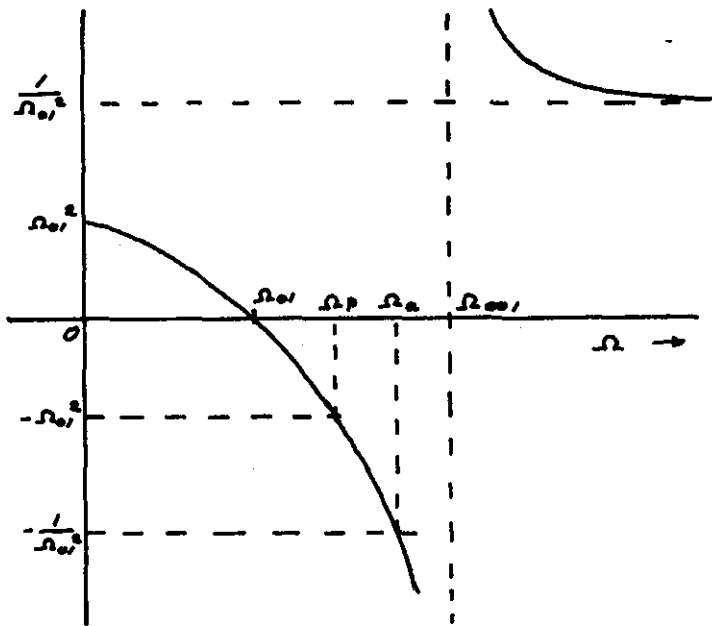


fig. 8.

From (12) we get $\mathcal{D}(0) = \Omega_{01}^2 = L$

Therefore

$$\Omega_{01} = \sqrt{L}$$

$$\text{and } \Omega_{\infty 1} = \sqrt[3]{L} \quad (13)$$

Then Ω_p follows from $\mathcal{D}(\Omega_p) = -\Omega_{01}^2 = -L$ giving

$$\left. \begin{aligned} \Omega_p &= \sqrt{\frac{2L}{1+L^2}} \\ \Omega_a &= \frac{1}{\Omega_p} \end{aligned} \right\} \quad (14)$$

From (14) the selectivity factor k defined by $k = \frac{\Omega_p}{\Omega_a} = \Omega_p^2$ becomes

$$k = \frac{2L}{1+L^2} \quad (15)$$

For quick reference k can be determined from fig. 9 for given D_p and D_a .

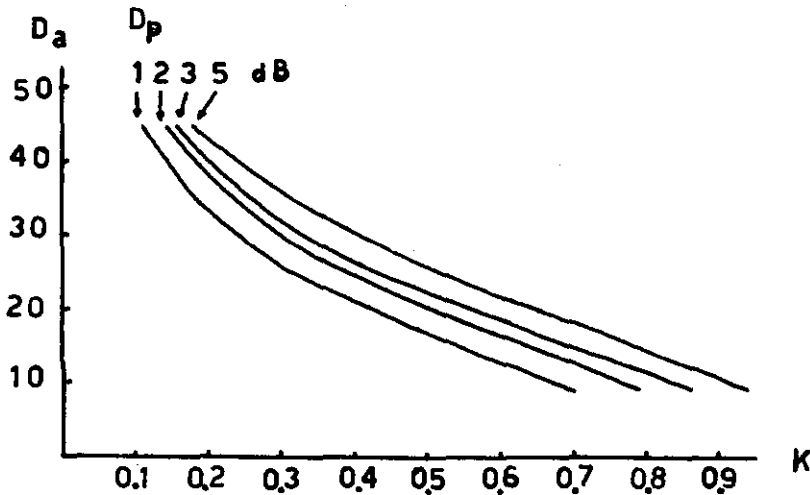


fig. 9.

The above formulas lead to the following design procedure

1. Determine from fig.9 if the given D_p and D_a will lead to a satisfactory selectivity factor k . Otherwise a higher order filter must be designed.
2. Calculate L and H from eq.(11).
3. $\mathcal{D}(\Omega)$ follows as

$$\mathcal{D}(\Omega) = \frac{\Omega^2 - \Omega_{01}^2}{\Omega^2 \Omega_{01}^2 - 1} \quad \text{with} \quad \Omega_{01} = \sqrt{L}$$

$|H(j\Omega)|^2$ is given by (1).

4. The various characteristic frequencies follow from (13) and (14).
5. Here or afterwards use a frequency transformation to obtain the desired values for the frequencies of point 4.

For a fourth degree approximation two terms in (10) are needed.

In order to simplify the calculation Ω_{02} is set equal to zero which appears to be equivalent to a certain frequency transformation operated on the normal fourth degree approximation leading to the so called "bar-type" filters in ref. [1]. At the same time this results in a zero in $|H(j\Omega)|$ as Ω approaches infinity.

So $\Phi(\Omega)$ becomes

$$\Phi(\Omega) = \Omega^2 \frac{\Omega^2 - \Omega_{01}^2}{\Omega^2 \Omega_{01}^2 - 1} \quad (16)$$

with its graph shown in fig. 10.

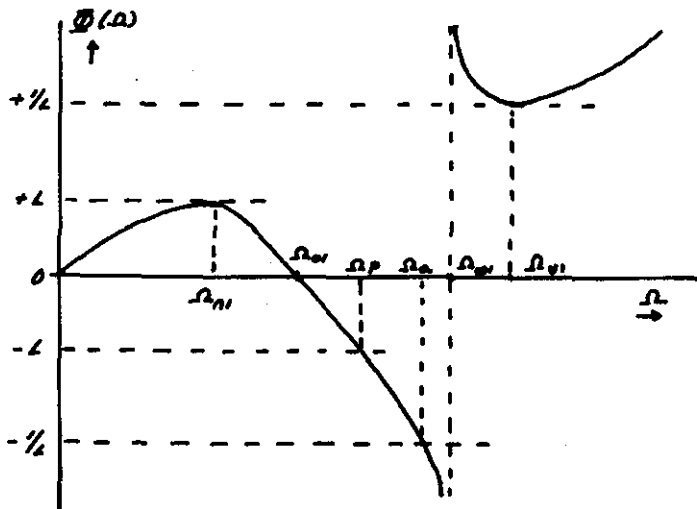


Fig. 10.

To derive Ω_{01} from (16) one proceeds as follows.

Ω_{01} is determined by the quadratic equation $\Phi(\Omega_{01}) = L$. Because $\Phi(\Omega)$ is tangential to the line $\Phi = L$ the previous quadratic equation has two coincident roots and therefore zero discriminant.

$\Phi(\Omega_{01}) = L$ with $\Omega_{01}^2 = x$ leads to

$$x^2 - \Omega_{01}^2(1+L)x + L = 0$$

Forcing the discriminant equal to zero gives

$$\Omega_{01}^4(1+L)^2 - 4L = 0 \quad \text{resulting in}$$

$$\Omega_{01} = \left[\frac{2\sqrt{L}}{1+L} \right]^{1/2} \quad (17)$$

and

$$\Omega_{01} = 1/\Omega_{01}$$

The solution of the quadratic equation becomes

$$x = \Omega_{01}^2 = \sqrt{L}$$

Therefore

$$\left. \begin{aligned} \Omega_{01} &= \sqrt[4]{L} \\ \text{and } \Omega_{01} &= 1/\sqrt[4]{L} \end{aligned} \right\} \quad (18)$$

At last Ω_p follows from

$$\begin{aligned} \Phi(\Omega_p) &= -L \text{ giving} \\ \Omega_p^2 &= \Omega_p/\Omega_a = k = \sqrt{L} \left[\frac{1-L}{1+L} + \sqrt{\left(\frac{1-L}{1+L}\right)^2 + 1} \right] \end{aligned} \quad (19)$$

In fig.11 the selectivity factor k is given in dependence from D_p and D_a .

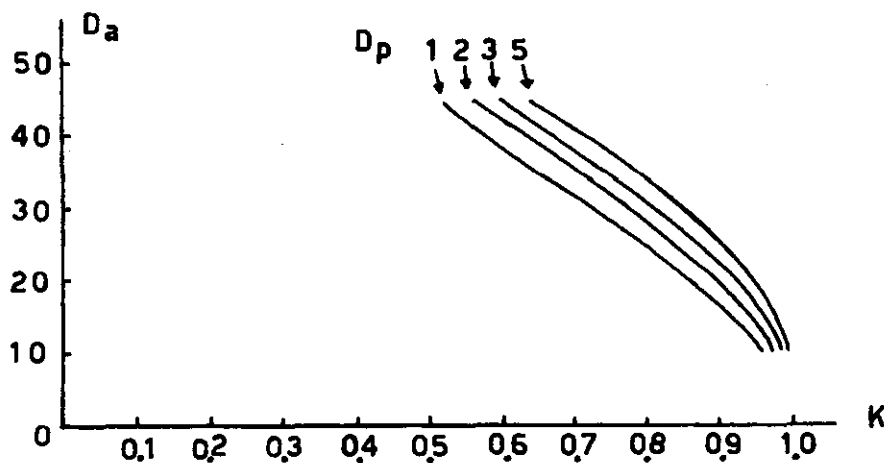


fig. 11.

Design procedure

1. Determine from fig.11 if the given D_p and D_a will lead to satisfactory selectivity factor k . Otherwise a higher order filter must be designed.
2. Calculate L and H from eq. (11).
3. $\Phi(\Omega)$ follows as

$$\Phi(\Omega) = \Omega^2 \frac{\Omega^2 - \Omega_{01}^2}{\Omega^2 \Omega_{01}^2 - 1} \quad \text{with} \quad \Omega_{01} = \left[\frac{2\sqrt{L}}{1+L} \right]^{1/2}$$

$|H(j\omega)|^2$ is given by (1)

4. The various characteristic frequencies follow from (17), (18) and (19).
5. Here or afterwards use a frequency transformation to obtain the desired values for the frequencies of point 4.

1.3.3 Derivation of the transferfunction from a given modulus.

The modulus of a transferfunction is determined by

$$|H(j\omega)|^2 = H(p) \cdot H(-p) \Big|_{p=j\omega} \quad (20)$$

This equation immediately shows that $|H(j\omega)|^2$ is an even function of ω , thus only approximations for $|H(j\omega)|^2$ with even functions can be tolerated.

Defining $H(p) = \frac{H(j\omega)}{|H(j\omega)|^2}$ we have from (20)

$$H\left(\frac{p}{j}\right) = H(p) \cdot H(-p) = Q(p) \quad (21)$$

Herein $Q(p)$ is a real rational and even function of p and can be obtained from $|H(j\omega)|^2$ by substituting $\omega^2 = -p^2$.

As $|H(j\omega)|^2 \geq 0$ this implies that $Q(p) \geq 0$ for imaginary p .

Therefore the zeroes and poles of $Q(p)$ on the imaginary axis must be of even multiplicity otherwise $Q(p)$ would change sign in these points.

The stability of $H(p)$ however requires the imaginary poles of $Q(p)$ to have multiplicity 2.

Because $H(p)$ is a real rational function of p , its complex poles and zeros arise in complex conjugate pairs. On account of (21) the complex poles and zeros of $Q(p)$ will then show quadrantal symmetry.

Real-axis poles and zeros of $Q(p)$ are each other mirror-images w.r.t. the imaginary axis.

As in the resulting $H(p)$ the poles must lie in the left half plane with single poles on the imaginary-axis to insure stability, we can construct $H(p)$ from the above

$Q(p)$ by assigning a pole-zero pattern to $H(p)$ consisting

of all the poles and zeros of $Q(p)$ in the left half-plane and half of its poles and zeros on the imaginary-axis. Then automatically $H(p) \cdot H(-p)$ has the same poles and zeros as $Q(p)$ because $H(-p)$ has the mirror-image pole-zero pattern of $H(p)$.

The in this way constructed $H(p)$ is called "minimum-phase" transferfunction.

1.3.4 Numerical example of a fourth-degree approximation.

Suppose one has to design a low-pass filter for use in telephone-links having the following specifications:

Passband edge-frequency 3400 c/s

Stopband edge-frequency 4500 c/s

Passband ripple 3 dB

Stopband ripple 30 dB

The design starts by calculating the prescribed selectivity factor k giving

$$k = \frac{\Omega_p}{\Omega_a} = \frac{2\pi \cdot 3400}{2\pi \cdot 4500} \approx 0.75$$

Following the five steps of chapter 1.3.2 results in:

sub.1. From fig.11 it can be seen that the given losses will lead to a selectivity-factor $k=0.81$ which is certainly better than the required $k=0.75$. (One may alter D_p or D_a to get closer to $k=0.75$ for example by taking $D_p = 2$ dB and $D_a = 30$ dB giving $k=0.78$).

sub.2. From (11) follows $L=0.1776$ and $H=5.6153$.

sub.3. (17) gives $\Omega_{o1} = 0.846063$ and $\Omega_{o2} = 1.181945$

This leads to

$$\Phi(\Omega) = \Omega^2 \frac{\Omega^2 - 0.0461^2}{\Omega^2 0.0461^2 - 1}$$

Then (1) gives

$$|H(j\Omega)|^2 = \frac{1}{1 + H^2 \Phi^2(\Omega)} = \frac{(0.72\Omega^2 - 1)^2}{31.53\Omega^8 - 45.14\Omega^6 + 16.67\Omega^4 - 1.43\Omega^2 + 1}$$

sub.4. From (18) and (19) follows

$$\begin{aligned}\Omega_p &= 0.90 & \Omega_{n1} &= 0.65 \\ \Omega_a &= 1.11 & \Omega_{n2} &= 1.54\end{aligned}$$

sub.5. The passband edge-frequency of sub.4 being $\Omega_p = 0.90$ has to be transformed to the desired one given by $\omega_p = 2\pi \cdot 3400 = 21363$ rad/sec.

Therefore a frequency transformation must be made by substituting

$$\Omega = \frac{0.90}{21363} \omega = 0.0000421 \omega \quad \text{in } |H(j\Omega)|^2$$

Its however more easy to make this transformation after the whole transferfunction is realised by changing the final elementvalues with a proper factor. In this way the calculation proceeds with coefficients and elements being of comparable value thereby reducing the chance on making errors in the computations.

For calculating $H(p)$ we find from (21)

$$Q(p) = \frac{(0.72p^2 + 1)^2}{31.53p^8 + 45.14p^6 + 16.67p^4 + 1.43p^2 + 1}$$

The poles of $Q(p)$ follow as the zeros of the above denominator giving

$$\begin{aligned}P_{1,2,3,4} &= \pm (0.06092 \pm j 0.86747) \\ P_{5,6,7,8} &= \pm (0.36631 \pm j 0.31825)\end{aligned}$$

The zeros of $Q(p)$ are found as

$$\begin{aligned}P_{1,2} &= \pm j 1.1819 \\ P_{3,4} &= \pm j 1.1819\end{aligned}$$

From the above we find the poles of $H(p)$ as

$$\begin{aligned}P_{1,2} &= -0.06092 \pm j 0.86747 \\ P_{3,4} &= -0.36631 \pm j 0.31825\end{aligned}$$

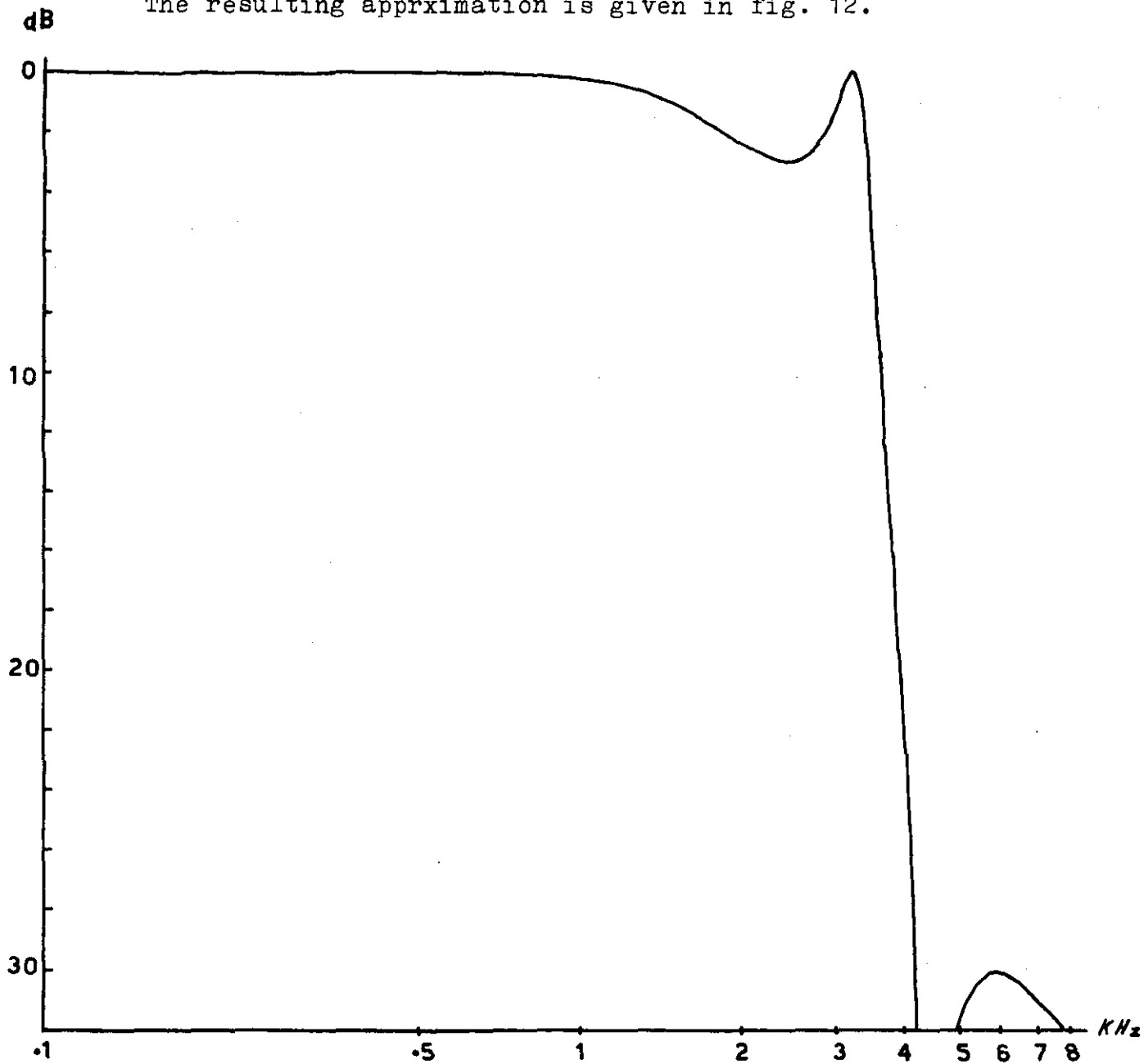
and its zeros as

$$p_{1,2} = \pm j 1.1819.$$

Then $H(p)$ becomes

$$H(p) = 0.17807 \frac{(0.7159 p^2 + 1)}{(p^2 + 0.12184p + 0.75622)(p^2 + 0.73262p + 0.23547)}$$

The resulting approximation is given in fig. 12.



2.1 Network sensitivity.

Any transferfunction of a network is as function of the network elements sensitive to element variations. The network structure capable to realize a certain transferfunction having the least sensitivity compared with other structures is thus the favourable one for use in the synthesis, because unavoidable tolerances in the element values will then have the smallest influence on the realised transferfunction.

It is then reasonable to use the sensitivity as a basic criterium in the network design, especially in active filter applications which can be very sensitive, in order to assure that the transferfunction can be realised with sufficient accuracy. For the comparison ~~of~~ ^{of} the various possible structures it is therefore necessary to have a measure for the sensitivity. Depending on the type of transferfunction and its application, various definitions are used, the most current of them given below.

1. Parameter sensitivity $S_r^{W(p,r)}$ defined as $S_r^{W(p,r)} = \frac{r}{W(p,r)} \frac{\partial W(p,r)}{\partial r}$

Here in $W(p,r)$ can be a transferfunction, transferloss, quality factor etc., with parameter r .

2. Pole- or zero-sensitivity S_r^q . If $q = \sigma(r) + j\Omega(r)$ is a pole or zero of some transferfunction, S_r^q is defined as

$$S_r^q = \frac{r}{\sigma} \frac{\partial \sigma}{\partial r} + j \frac{r}{\Omega} \frac{\partial \Omega}{\partial r}$$

The following derivation may simplify the application of the loss-sensitivity.

As $\alpha = -10 \log |H(j\omega)|^2$ we have

$$\begin{aligned} S_r^\alpha &= \frac{r}{\alpha} \frac{\partial [-10 \log |H(j\omega)|^2]}{\partial r} = -\frac{10}{\ln 10} \frac{r}{\alpha} \frac{1}{|H(j\omega)|^2} \frac{\partial |H(j\omega)|^2}{\partial r} \\ &= \frac{-10}{\alpha \ln 10} S_r^{|H(j\omega)|^2} = -\frac{4.34}{\alpha} S_r^{H(p) \cdot H(p)} \Big|_{p=j\omega} \end{aligned} \quad (22)$$

From the definition we can derive

$$S_r^W(p) \cdot V(p) = S_r^W(p) + S_r^V(p)$$

With (22) this results in

$$S_r^d = - \frac{4.34}{\alpha} [S_r^{H(p)} + S_r^{H(\omega)}] \Big|_{p=j\omega}$$

leading to

$$S_r^d = - \frac{0.68}{\alpha} \operatorname{Re} [S_r^{H(j\omega)}]$$

Approximating S_r^d with $\frac{r}{\alpha} \frac{\Delta \alpha_r}{\Delta r}$ we finally have

$$\left. \begin{aligned} \Delta \alpha_r &= - 0.68 \operatorname{Re} [S_r^{H(j\omega)}] \cdot \frac{\Delta r}{r} \text{ dB} \\ \text{or } \Delta \alpha_r &= - \operatorname{Re} [S_r^{H(j\omega)}] \cdot \frac{\Delta r}{r} \text{ Neper.} \end{aligned} \right\} \quad (23)$$

2.2.1 Sensitivity functions for second-order low-pass LC^R-filters.

In active synthesis a frequently used method consists in dividing a transferfunction in second order parts with parts are then realized with suitable active circuits and cascaded by inserting isolation amplifiers if necessary. The overall sensitivity of the resulting network then depends on the partial sensitivity of these second order sections. It is therefore convenient to compare the active second order filter sensitivities with those of a passive one realising the same transferfunction, because we have a lot of practical experience with this filter type and need a reference anyway.

Let the passive equivalent be given as in fig. 13.

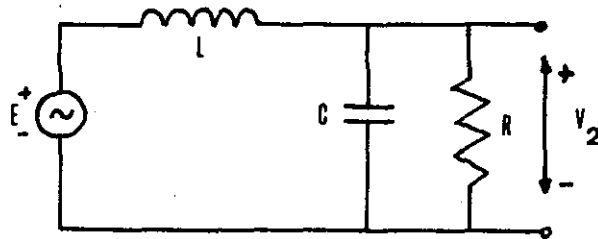


fig. 13.

A straight-forward calculation shows the voltage transferfunction to be

$$H(p) = \frac{V_2}{E} = \frac{1}{p^2 LC + \frac{L}{pR} + 1} \quad (24)$$

From (24) the following poles results:

$$P_{1,2} = -\frac{1}{2RC} \pm j \sqrt{\frac{1}{LC} - \left(\frac{1}{2RC}\right)^2} \quad \text{if } R > \frac{1}{2} \sqrt{L/C}$$

With

$$\sigma = -\frac{1}{2RC}, \quad \omega_0 = \frac{1}{\sqrt{LC}} \quad \text{and } Q = R \sqrt{C/L} \quad \text{this becomes}$$

$$P_{1,2} = \sigma \pm j \omega_0 \sqrt{1 - (1/2Q)^2} \quad \text{with } Q > 1/2$$

This leads to the following pole-sensitivities:

$$\left. \begin{aligned} S_C^P &= -1 - j \cdot \frac{1}{2} \frac{1 - 1/4Q^2}{1 - 1/4Q^2} \approx -1 - j \left(\frac{1}{2} - \frac{1}{4Q^2} \right) \\ S_L^P &= -j \frac{1/2}{1 - 1/4Q^2} \approx -j \left(\frac{1}{2} + \frac{1}{4Q^2} \right) \\ S_R^P &= -1 + j \frac{1}{4Q^2 - 1} \approx -1 + j \cdot 1/4Q^2 \end{aligned} \right\} \quad (25)$$

More over the Q-factor sensitivity as well as the resonant-frequency sensitivity follow as

$$\left. \begin{aligned} S_C^Q &= 1/2 \\ S_L^Q &= -1/2 \quad \text{and} \quad S_{\omega_0}^{\omega_0} = S_C^{\omega_0} = -1/2 \\ S_R^Q &= 1 \quad \quad \quad S_{\omega_0}^R = 0 \end{aligned} \right\} \quad (26)$$

Calculating the loss sensitivity one finds

$$S_C^{H(\omega)} = \frac{c}{H(\omega)} \cdot \frac{\partial H(\omega)}{\partial C} \Big|_{\omega=j\omega} = \frac{\omega^2 LC}{1 - \omega^2 LC + j\omega^2/R}$$

Normalising the frequency ω to the resonant frequency ω_0 by substituting $\Omega = \frac{\omega}{\omega_0}$ we find:

$$S_C^{H(\Omega)} = \frac{\Omega^2}{1 - \Omega^2 + j \frac{R}{Q}}$$

Then (23) results in

$$\Delta \alpha_C = -\text{Re} \left[S_C^{H(\Omega)} \right] \cdot \frac{\Delta C}{C} = \frac{-\Omega^2 (1 - \Omega^2)}{(1 - \Omega^2)^2 + \frac{\Omega^2}{Q^2}} \cdot \frac{\Delta C}{C} \quad \text{Neper}$$

In the same way we find

$$\Delta \alpha_R = \frac{-\Omega^2/Q^2}{(1 - \Omega^2)^2 + \Omega^2/Q^2} \cdot \frac{\Delta R}{R} \quad \text{Neper}$$

and

$$\Delta \alpha_L = \frac{-\Omega^2 (1 - \Omega^2) + \Omega^2/Q^2}{(1 - \Omega^2)^2 + \Omega^2/Q^2} \cdot \frac{\Delta L}{L} \quad \text{Neper}$$

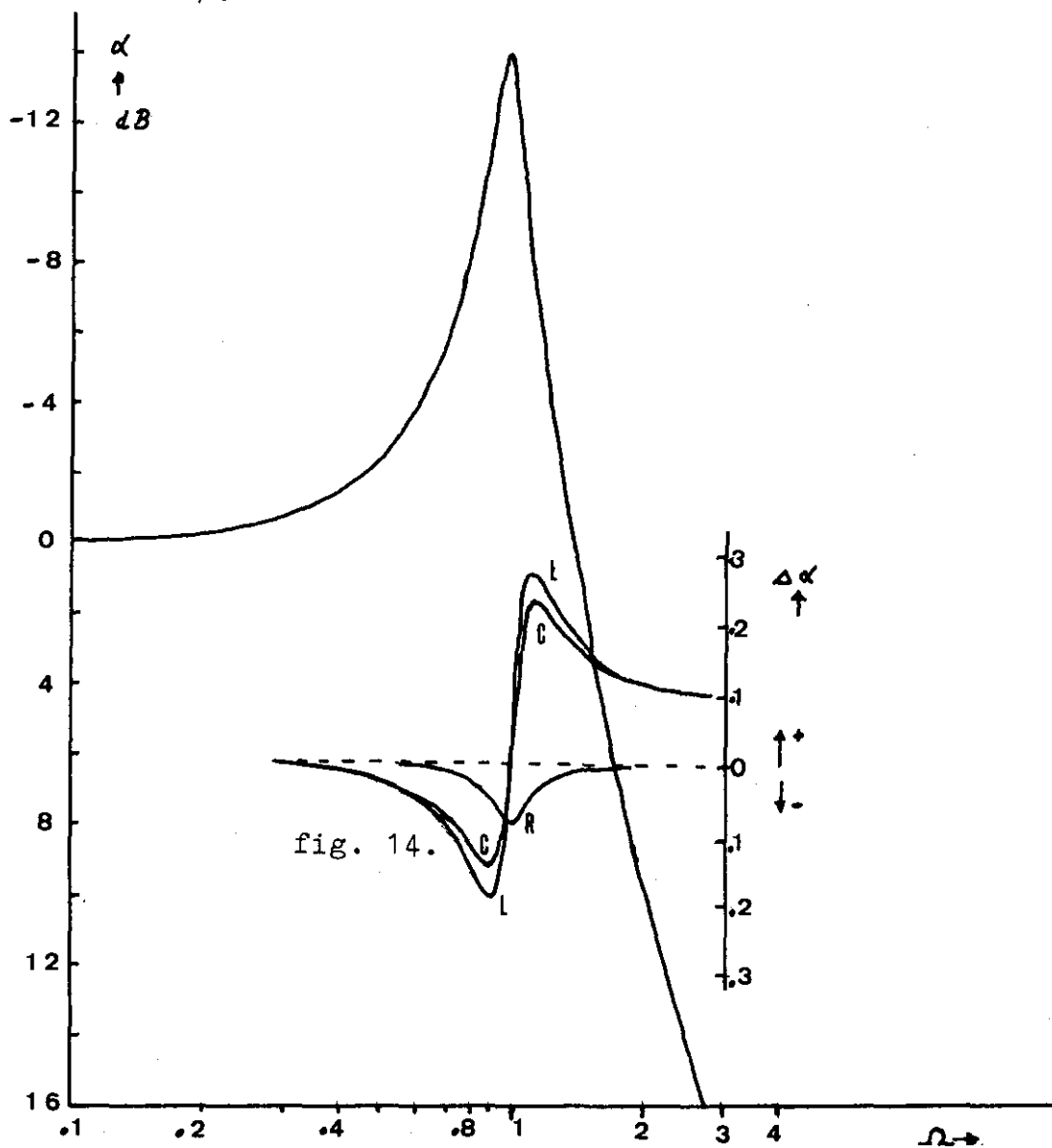
The maximum values of these loss-variations for large Q-factor become

$$\Delta \alpha_C \text{ max} \approx \pm \frac{Q}{2} \cdot \frac{\Delta C}{C} \text{ Neper}$$

$$\Delta \alpha_L \text{ max} \approx \pm \frac{Q}{2} \cdot \frac{\Delta L}{L} \text{ Neper}$$

$$\Delta \alpha_R \text{ max} \approx -7 \cdot \frac{\Delta R}{R} \text{ Neper}$$

The above variations are shown together with the normalised transferloss α in fig. 14 for $Q = 5$ and element variation 1%.



2.2.2 Sensitivity calculation for an active second-order low-pass filter

Consider the active filter in fig. 15 where in the operational amplifiers are supposed to be ideal.

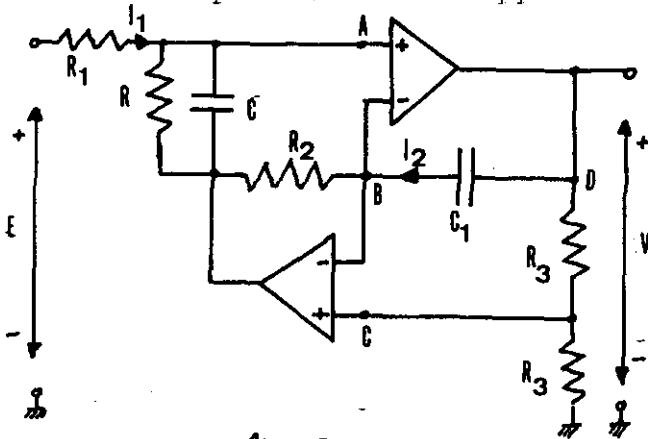


fig. 15

This results in the same potential for the points A, B and C.

The potential-divider R_3-R_3 gives $V_C = \frac{V_D}{2} = \frac{V}{2}$

Therefore $V_B = \frac{V}{2}$ and

$$i_2 = \frac{V_D - V_B}{1/pC_1} = \frac{pC_1}{2} \cdot V$$

This current i_2 flows into the resistor R_2 re-

sulting in a voltage drop over R_2 given by

$$\Delta V = R_2 i_2 = \frac{pC_1 R_2}{2} \cdot V$$

Because $V_A = V_B$ the same voltage-drop must fall over the parallel combination $R-C$ hence the current flowing through it follows as

$$i_1 = \frac{1+pRC}{R} \cdot \frac{pR_2 C_1}{2} \cdot V.$$

On the other hand V_A is given by

$$V_A = E - R_1 i_1 = \frac{V}{2}.$$

Substituting i_1 in this formula and solving for $\frac{V}{E}$ gives

$$\frac{V}{E} = \frac{2}{p^2 R_1 R_2 C_1 C + p \frac{R_1 R_2 C_1}{R} + 1} \quad (27)$$

If we take $R_1 R_2 C_1 = L$ we find formula (27) except for a constant factor to be exactly equal to formula (24) which resulted from the passive filter in fig. 13.

Therefore we can conclude immediately that the sensitivities for the active filter given here are the same as those of the passive one dealt with in the previous chapter if we make the following correspondence:

$$\left. \begin{aligned}
 S_{b R_1}^W &= S_{b R_2}^W = S_{b C_1}^W = S_a^W L \\
 S_{b C}^W &= S_a^W C \quad \text{and} \quad S_{b R}^W = S_a^W R
 \end{aligned} \right\} \quad (28)$$

Here in the index a refers to the network of fig. 13 where as the index b refers to the active network.

As in the case of the passive filter, this active filter is always stable for every positive value of the elements. The root-locus is therefore confined to the left half-plane. Furthermore (27) and (28) indicate that this active filter only differs from the passive one in the sensitivity w.r.t. the equivalent L being three-fold instead of a simple one. The influence due to the non-ideality of the amplifiers such as finite gain etc., is kept out of considerations because this influence is small if the amplifier bandwidth is taken to be large enough i.e. exceeding the frequencies of interest for the filter.

A sure advantage over the passive filter however is that any impedance may be connected to the output terminals without the transferfunction being changed. For this reason this filter type is very well applicable in cascade-synthesis.

2.2.3 Sensitivities for the Fjälbrant-filter.

The Fjälbrant-filter [3] or Sallen and Key filter in fig. 16 is another active filter capable to realize second-order transferfunctions however with much larger sensitivities than the foregoing one, in such a way that this filter can only be used when low to moderate Q-factors are dealt with.

From fig. 16 we easily calculate

$$H(p) = \frac{V_2}{E} = \frac{1}{p^2 R_1 R_2 C_1 C_2 + p \cdot [(1-A)R_1 C_1 + (R_1 + R_2)C_2] + 1}$$

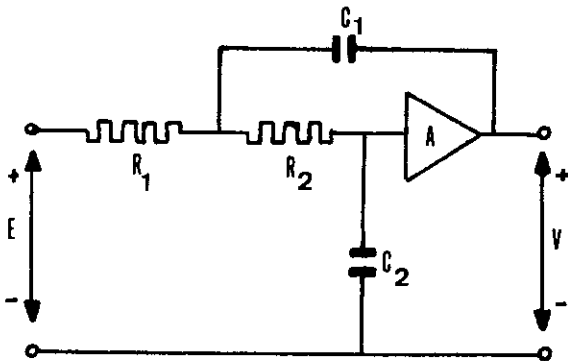


fig. 16.

A close look on the above transferfunction shows that in the case that A becomes large the coefficient of P may become negative, resulting in right half-plane poles and thus H(p) becomes unstable as can be seen from the root-locus of fig. 17 with arrowdirection corresponding to increasing A.

From H(p) the sensitivities are computed as

$$\left. \begin{aligned} S_A^Q &= A Q \sqrt{\frac{R_1 C_1}{R_2 C_2}} \\ \Delta \alpha_{R_{max}} &= 2 Q \frac{\Delta A}{A} \text{ Neper} \end{aligned} \right\} \quad (29)$$

If the values of (29) are compared with those of the passive filter we find them to be much greater. Especially S_A^Q becomes large for moderate Q-factor because in this case $\sqrt{\frac{R_1 C_1}{R_2 C_2}} \approx Q$ leading to $S_A^Q \approx A Q^2$.

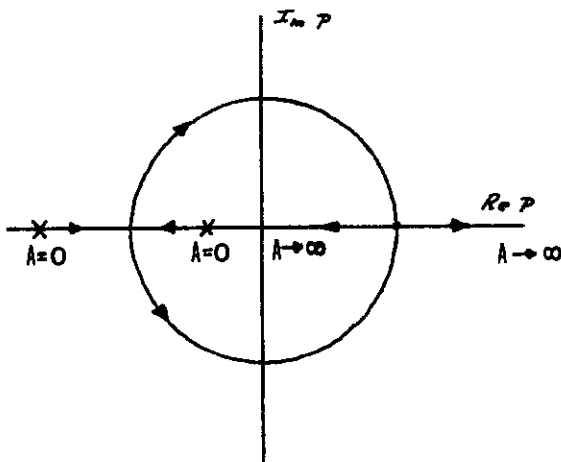


fig. 17.

On the basis of the foregoing comparison we have shown that active filters realising the same transferfunction can have different sensitivities, possibly being equal to or better than the passive ones as well as being worse. ^{f Generally} Only low sensitivities will guarantee good agreement between the wanted and really obtained

transferfunctions. Hence one should prefer the slight more complicated network of fig. 15 above the Fjälbrant-filter when moderate or high Q-factors are needed.

However large pole-sensitivity does not always imply large filterloss sensitivity as can be seen from equations (25). If we take $Q \approx \frac{1}{2}$, we find $S_c^p \approx -1-j\infty$ indicating that the pole-sensitivity becomes very large due to the large relative change in the imaginary part. The filterloss for small Q-factors is however mainly determined by the real part of the poles and is therefore much less sensitive to element variations as one would expect from the large value of S_c^p . On the other hand small pole-sensitivity is not always coupled with small loss-sensitivity but in most cases the lower the sensitivities are, the better the filter will be as to the influence of parameter changes.

If the filter poles are determined by a difference of two polynomials each with positive coefficients, the resulting polynomial shows large coefficient sensitivity for the smallest coefficients because these coefficients are obtained by subtracting almost equal large numbers from each other. Therefore one must avoid synthesis methods leading to coefficients which are determined by a difference of products of the element values.

However if every polynomial coefficient consists only of the sum of products of the element values, the filter still can be very sensitive to element variations. For example the polynomial $p^3+p^2+1,01p+1$ is a Hurwitz polynomial while $p^3+p^2+0,99p+1$ has zeros in the right half plane and thus leads to instability if this polynomial would determine the poles of a transferfunction. Hence a slight change of one coefficient due to a change in one of its composing products may result in instability even if this coefficient is build up with positive sums of these products.

On account of the foregoing one may conclude that the sensitivity plays an important role in the design of stable and insensitive networks but large or small sensitivities on their own are not absolute criteria for the behaviour of the designed filter.

3.1 Active filters obtained by substitution methods.

The synthesis of active filters will solely involve known methods if they can be derived from the passive filters in some direct way. In this case one uses passive synthesis methods to construct active filters by changing the passive filter so as to eliminate the appearing inductances.

The mainly used methods hereto are replacement of the inductors by gyrators and capacitors as explained in the following section and impedance transformation as will be given in section 3.3.

3.2.1 Gyrator-capacitor substitution.

Consider the circuit of fig. 18 where in the gyrator is defined by the following non-reciprocal two-port admittance-matrix

$$[Y] = \begin{bmatrix} 0 & G \\ -G & 0 \end{bmatrix} \quad \text{with } G = 1/R \text{ } [\Omega^{-1}] \quad (30)$$

Connecting an admittance y_L to the port 2-2' gives an input admittance

$$y_{in} = y_{11} + \frac{y_{12} y_{21}}{y_{22} + y_L} = \frac{G^2}{y_L}$$

Especially for $Y_L = PC$ we get $Y_{in} = \frac{G^2}{PC} = \frac{1}{pR^2C}$, being the admittance of an inductor with inductance $L = R^2C$ Henry. Therefore this configuration can be used to replace inductors in a passive LCR filter. As an example a third-order Butterworth low-pass filter is then realised as depicted in fig. 19.

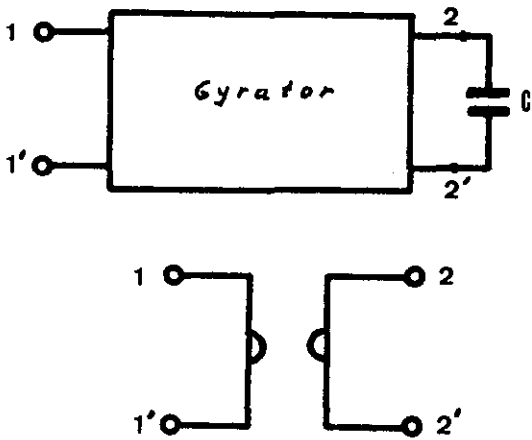


fig. 18.

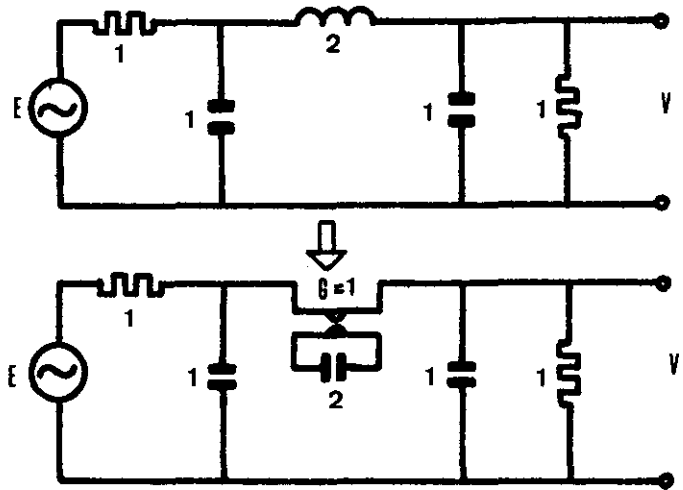


fig. 19.

On sensitivity point of view this network only differs from the original LCR-filter in the sensitivity due to elements in the capacitor-gyrator circuit.

As was indicated by ^{Orchard} ~~Piordan~~ [4] this leads to low-sensitivity of the resulting network as compared with other active circuits with the general tendency as to shift the poles further away from the imaginary axis. Hence the network is always stable.

3.2.2 Gyrator circuits.

For the gyrator to have good quality, i.e. approaching (30) as much as possible, one uses electronic circuits to construct it. The main point of interest lies in the diagonal elements of (30) which must become as close to zero as possible however remain positive. To demonstrate this point consider the non-ideal gyrator admittance-matrix

$$[y] = \begin{bmatrix} G_1 & G_2 \\ -G_3 & G_4 \end{bmatrix}$$

Connecting a capacitance pC_2 between the output terminals gives an input admittance

$$Y_{in} = G_1 + \frac{G_2 G_3}{G_4 + pC_2}$$

The equivalent circuit for this admittance is given in fig.20.

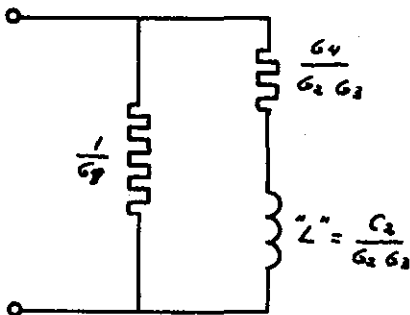


fig. 20.

It can be seen directly that this circuit approaches the ideal inductance the better if G_1 and G_2 approach zero. They must however remain positive otherwise the admittance becomes unstable as poles or zeros may arise in the right half-plane. We also see that G_2 not necessary has to be equal to G_3 .

Further on placing a capacitor C_1 across the input terminals results in a resonant circuit. The maximum obtainable Q-factor can be computed as $Q_{\max} = \frac{1}{2} \sqrt{1 + \frac{G_2 G_3}{G_1 G_4}}$ if $\frac{C_1}{C_2} = \frac{G_1}{G_4}$ is satisfied.

These results are the same as using an ideal gyrator and two non-ideal capacitors with parallel conductance G_1 and G_2 . The relation $\frac{C_1}{C_2} = \frac{G_1}{G_2}$ then implies equal Q-factor for

the capacitors and hence $Q_{\max} = \frac{1}{2} Q_c$. As for the frequently used polyester-capacitors with $\epsilon \approx 0.0004$ we have

$Q_c = \frac{1}{\epsilon} \approx 2500$ and find the maximum obtainable Q-factor to be $Q_{\max} \approx 1250$. This Q-factor will be reduced further because the gyrator will be non-ideal but is still much greater than the Q-factors obtainable with passive inductors.

The gyrator circuit given in fig. 21 is an example of a circuit ~~where~~ ^{with} in compensation with a negative resistor is used to force the diagonal elements of the admittance-matrix to zero and is as a consequence from the foregoing only suitable for realising low Q-factor inductancies, by assuring Y_{11} and Y_{22} to be positive (i.e. by conscious undercompensation).

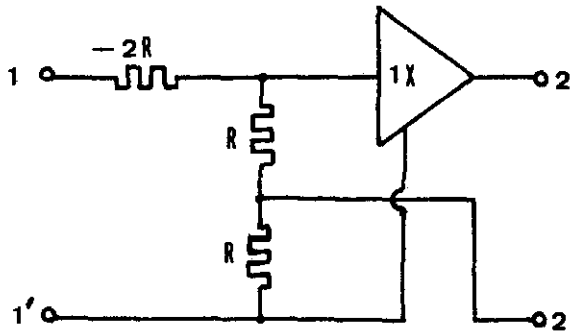


fig. 21.

A better circuit can be obtained from this one if the negative resistor is replaced by a feedback loop as depicted in fig.22. This results in an admittance-

$$[y] = \begin{bmatrix} 0 & G_1 \\ -G_2 & \frac{G_1 + G_2}{1 + S/G_2} \end{bmatrix}$$

If furtheron $S/G_2 \gg 1$ this becomes

$$[y] = \begin{bmatrix} 0 & G_1 \\ -G_2 & \frac{(G_1 + G_2)G_2}{S} \end{bmatrix}$$

The latter shows that Y_{22} is always positive and can be made small enough by taking S sufficiently large and at the same time G_2 may be put to zero.

Because of the finite input impedance of T_1 and T_2 the value of Y_{11} will not be exactly zero but can be made small enough.

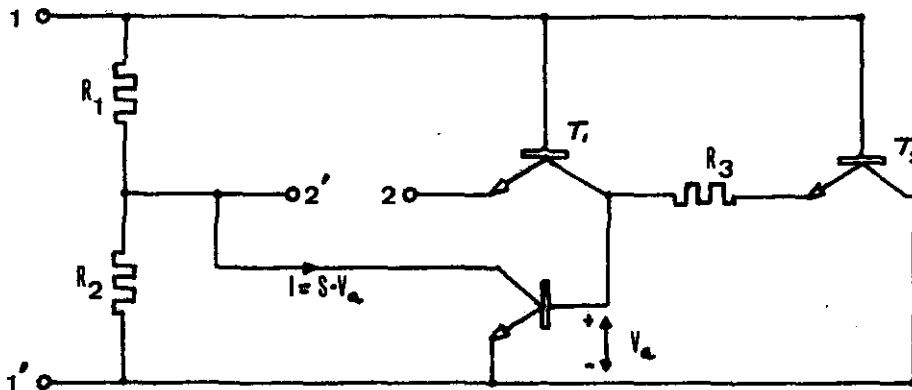


fig. 22.

A suitable practical circuit can be obtained from fig. 22 by rearranging its nullator-norator equivalent so as to produce a circuit with operational amplifiers instead of the given transistors. With the nullator-norator equivalence $[s]$ of the ideal transistor and operational amplifier given in fig. 23 this step is indicated in fig. 24.

From the last scheme in this fig. we obtain the practical circuit of fig. 25 as was first given by Riordan [6] .

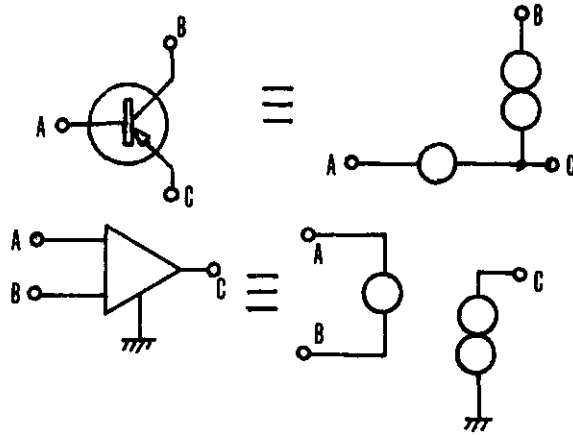


fig. 23.

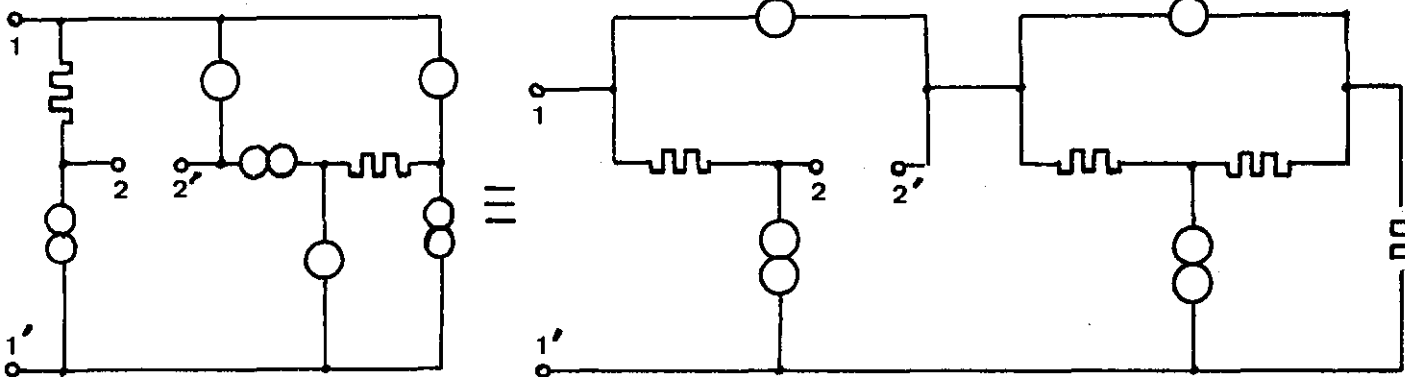


fig. 24.

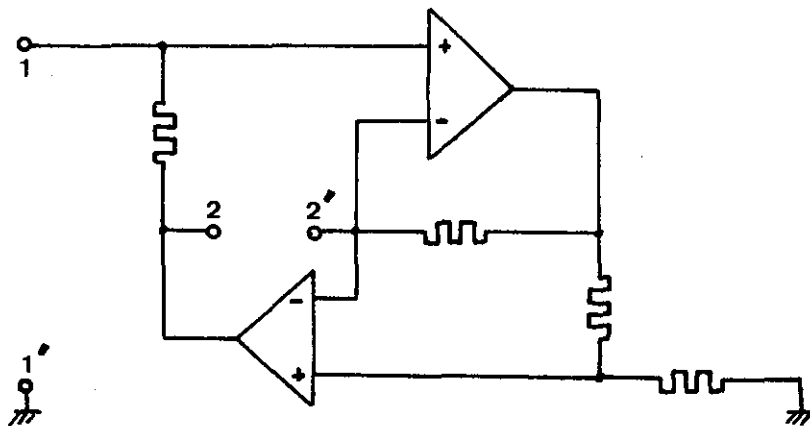


fig. 25.

There remains however the important disadvantage for these circuits not being able to realise "floating" inductors with one gyrator because of the galvanic coupling between in- and output-port.

Some alternative gyrator circuits are based on the two current source equivalent depicted in fig. 26 as follows from the decomposition of (30) in

$$[y] = \begin{bmatrix} 0 & g \\ 0 & 0 \end{bmatrix} + \begin{bmatrix} 0 & 0 \\ -g & 0 \end{bmatrix}$$

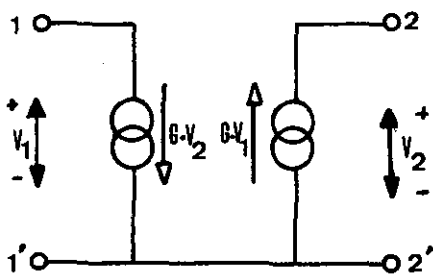


fig. 26.

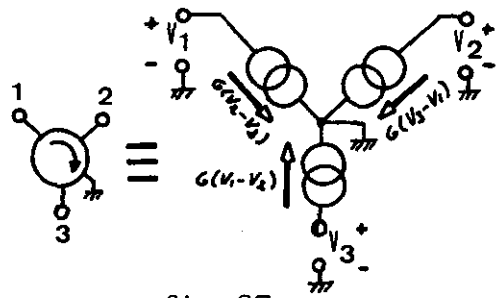
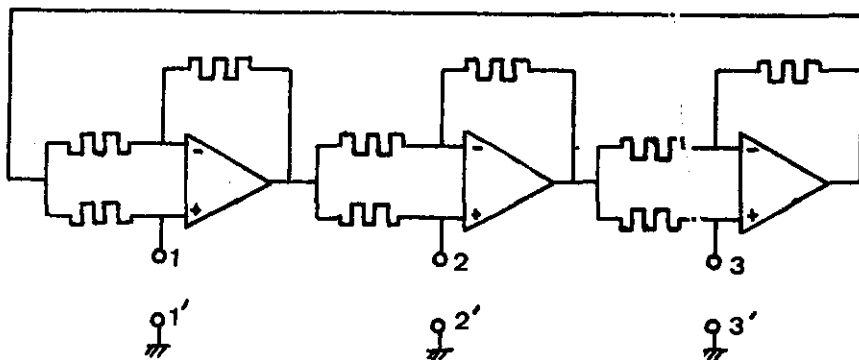


fig. 27.

Mr Creemers of the Technologic^{al} University Eindhoven has designed and actually constructed a circulator circuit with voltage controlled current sources given in fig. 27. Connecting a capacitor between the nodes 2 and 3 will give a floating inductance between node 1 and 2. However this circuit can become instable too if the admittances G_1 , G_2 and G_3 are different from each other.

At last the circuit of fig. 28 as given by Keen [7] can be used as a circulator and suffers from the same ^{dis-}advantage as the one in fig. 27, however the large gain of the amplifiers used in this structure assures its behaviour almost completely to be determined by the value of the resistors, which can be made sufficiently accurate to guarantee stable operation for Q-factors up to 500.



All resistors
with value R.
have a

fig. 28.

3.3 Active synthesis using frequency dependent negative resistors [6]

Consider the transmissionmatrix of an LCR two-port with parameters A, B, C and D. The voltage transferfunction of this two-port given by A is an imittance ratio and does not change when the admittancies in the network are scaled with a certain factor. This point opens the possibility to remove inductances by scaling all admittancies in the LCR two port with a factor p.

In that case we find the general admittance $Y = G + pC + \frac{1}{pL}$ to be changed to $Y^1 = pG + p^2C + \frac{1}{L}$. This implies that a conductance G will be transformed to a capacitance pG and an inductance pL will be transformed to a conductance $\frac{1}{L}$. However a capacitance pC will lead to an admittance p^2C being a frequency dependent negative resistor (FDNR) for $p = j\omega$. Hence we need an active circuit to realise the FDNR and use these elements together with resistors and capacitors for realising the transformed network.

Such an active FDNR is given in fig. 29 together with its representing symbol. Inherent to the configuration of this FDNR only grounded FDNR's can be realised. Hence this substitution-method will only work properly if the original network does not contain floating capacitors.

As the mid-series type LCR filter fullfills this requirement one tries to realise the passive filter in this form and afterwards derives the active circuit by the foregoing transformation.

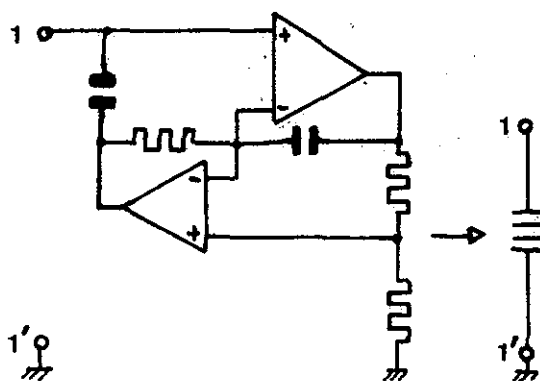


fig. 29.

As an example consider fig. 30, where this transformation is shown in detail. A disadvantage of this realisation lies in the output voltage going to zero as $\omega \rightarrow 0$. This is due to the finite input impedance of the operational amplifiers in the FDNR. However if the original network is designed as to have only inductors in the generator-branch this will result in resistors in series with the generator in the transformed network thus leading to the right low frequency response.

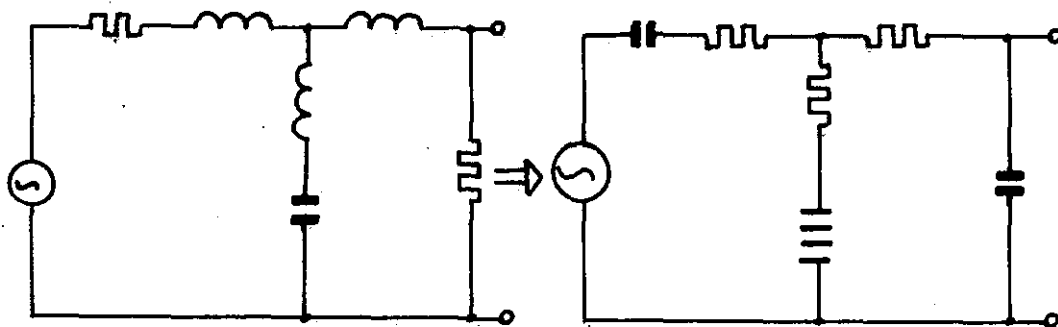


fig. 30.

As the FDNR is basically a positive immittance convertor (PIC) the resulting networks have an overall sensitivity comparable with other PIC-methods, which are claimed to be low.

As a fact the FDNR is realised by means of a PIC as depicted in fig. 31. Here in the generalised PIC is a two-port defined by the relations

$$\begin{aligned} V_1 &= V_2 \\ I_1 &= H(p)I_2 \end{aligned} \quad (29)$$

A realisation for the PIC is shown in fig. 32 with

$$H(p) = \frac{Z_2(p)Z_4(p)}{Z_1(p)Z_3(p)}$$

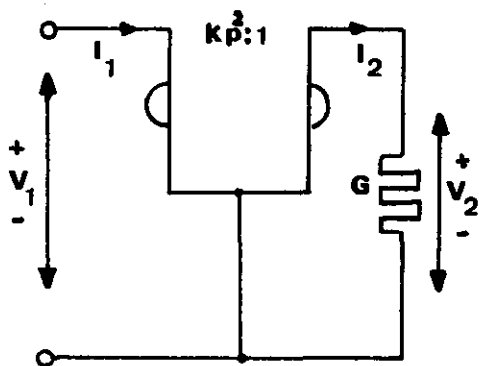


fig.31.

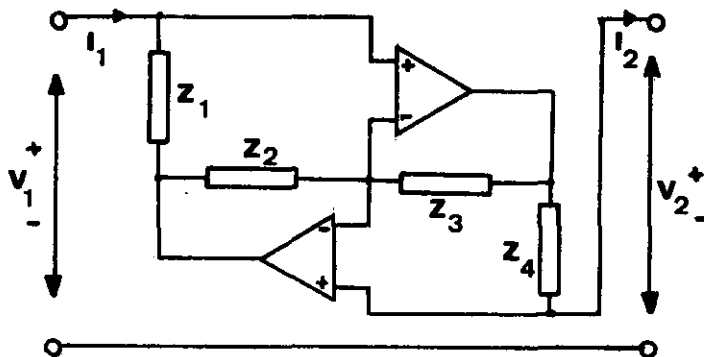


fig.32.

Taking $Z_1(p) = \frac{1}{pC_1}$, $Z_3(p) = \frac{1}{pC_2}$, $Z_2(p) = R_1$ and $Z_4(p) = R_2$ gives:

$$H(p) = k p^2 \text{ with } k = C_1 C_2 R_1 R_2$$

From (29) follows $\frac{I_1}{V_1} = H(p) \frac{I_2}{V_2}$ hence connecting an admittance Y to the secondport results in an input admittance $Y_{in} = H(p) \cdot Y$. Returning to fig. 31 we find $Y_{in} = kp^2 Y = kp^2 G$ being a FDNR and the resulting schematic diagram becomes that of fig. 29.

With these PIC's we can also simulate inductors directly as can be seen from fig. 33, leading to an input-impedance $Z = \frac{kp}{G}$ corresponding to an inductor "L" = $\frac{k}{G}$. In fact only one capacitor is used in this PIC and if we would redraw the schematic diagram in fig. 33 in such a way that the nodes where to the capacitor is connected would form the second port instead of 2-2', the resulting circuit would appear to be the gyrator given in fig. 25. Therefore replacing inductors by gyrator-capacitor circuits is equivalent to replacement by PIC's

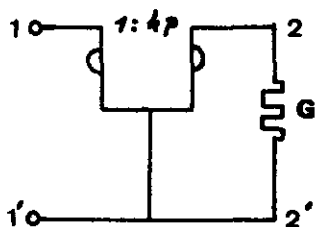


fig.33.

A floating inductor is in this case realised as shown in fig. 34 requiring the PIC's to ~~have~~ exactly reciprocal ~~current transfer ratios~~ in order to avoid ~~permissible tolerance~~ ~~to earth~~. *Nonreciprocal behaviour is for the equivalent two-port.*

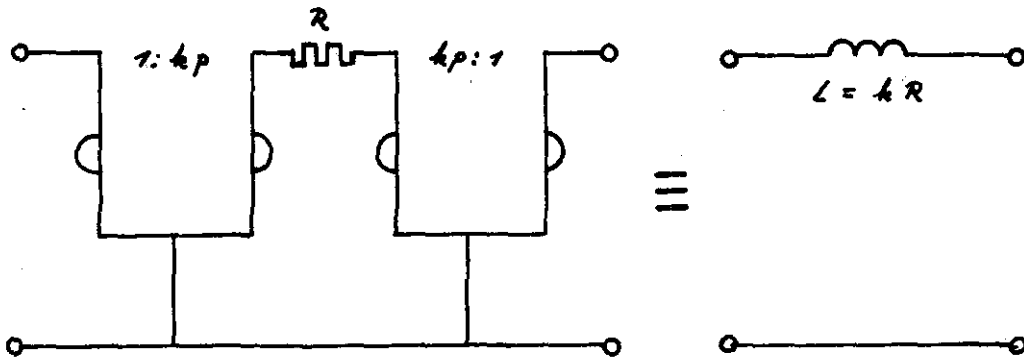


fig. 34.

In fig. 35 an example of this substitution method is depicted.

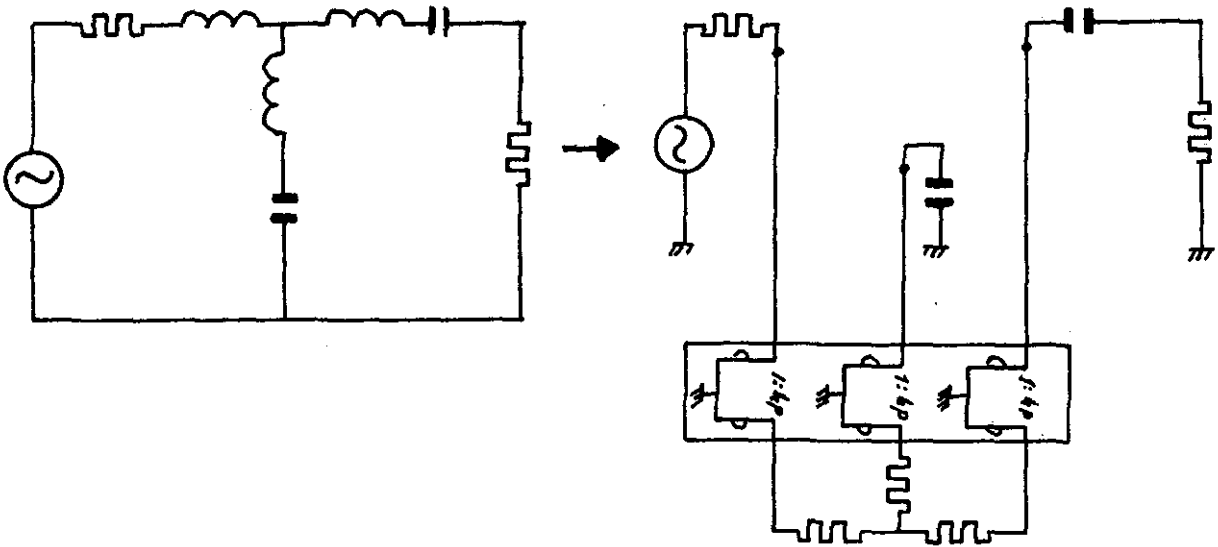


fig. 35.

The block with PICs performs a transformation as indicated by the following.

Consider a resistive network with impedance-matrix Z connected to a block of PICs as given in fig. 35.

For the resistive network holds $V = ZI$ with $V = \begin{pmatrix} v_1 \\ \vdots \\ v_m \end{pmatrix}$ and $I = \begin{pmatrix} i_1 \\ \vdots \\ i_m \end{pmatrix}$

The PICs give:

$$V' = V \text{ and } I' = \frac{1}{kp} I \text{ with } V' = \begin{pmatrix} v_1' \\ \vdots \\ v_m' \end{pmatrix} \text{ and } I' = \begin{pmatrix} i_1' \\ \vdots \\ i_m' \end{pmatrix}$$

Therefore ~~$V = ZI$~~ , $V' = V = Z \cdot I = kp Z I'$,

resulting in an impedance matrix for the nodes $1', 2', \dots, n'$ given by $Z' = kpZ$.

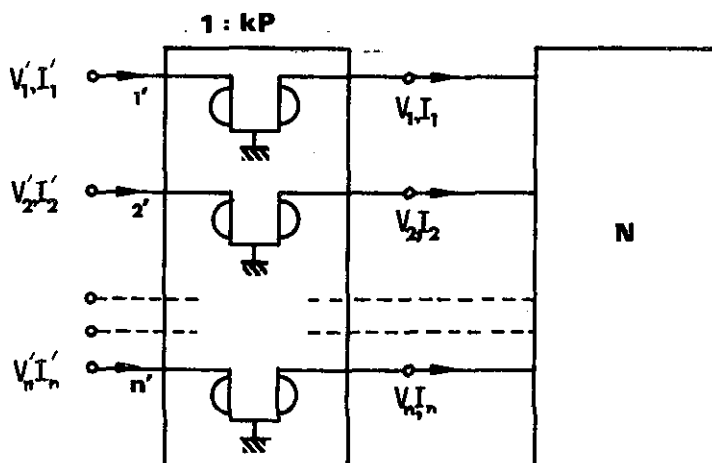


fig. 35.

Hence the network between these nodes is an inductive network with the same topological structure as the resistive network in which every inductance L_i has a value determined by $L_i = kR_i$ with R_i being the corresponding ~~Resistor~~^{ance} value in network N .

As these PICs have basically a gyrator structure and perform the same substitution, this method will result in the same low sensitivities as for the gyrator-capacitor substitution and in advantage over them they have the possibility to replace more inductors with less PICs on account of the above derivations. Furthermore for constructing floating inductors with gyrators, one needs a type with one common input-output node and until now no such circuit is known with a simplicity comparable with the above PIC-circuit. Hence we may conclude that the PIC-substitution is most favourable, leading to active networks with sensitivities comparable with those of the passive networks from which they are derived, while only known passive synthesis methods are involved to design the active filter.

4. Active filters on synthesis basis.

The active filters considered in this section have the property that the impedance matrix of the embedded networks can be derived from the original transferfunction by means of a general method in such a way that these former networks become realizable RC networks.

The structures given in chapter 4.1, 4.2 and 4.4 can realize every stable rational transferfunction, where as the gyrator-RC structure in chapter 4.3 is limited to certain filter classes.

4.1 Negative Impedance Converter (NIC) Synthesis.

One of the first available active filter structures given by Linvill uses a NIC in conjunction with two RC networks for realising transferfunctions. The basic configuration is depicted in fig. 36, in which the current-inversion NIC is shown between the dotted lines.

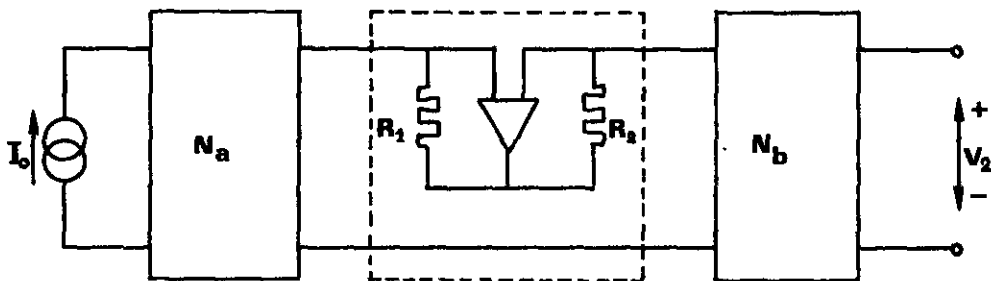


fig. 36.

With $\frac{R_1}{R_2} = k$ we find the chain-matrix of the NIC as

$$[K] = \begin{bmatrix} 1 & 0 \\ 0 & -k \end{bmatrix}$$

With this chain-matrix, the transferfunction of the above structure is given by

$$\frac{V_2}{I_0} = \frac{Z_{21}^b \cdot Z_{21}^a}{Z_{11}^b - k Z_{22}^a} \quad (30)$$

The realization of a given transferfunction proceeds as follows.

Let $H(p)$ be written as

$$H(p) = \frac{N(p)}{D(p)}$$

with $N(p)$ and $D(p)$ polynomials in p . As a first step divide the numerator and denominator of $H(p)$ by an arbitrary polynomial $Q(p)$ with its zeros on the negative real axis and degree $Q(p)$ equal to the maximum of the degree of $N(p)$ or $D(p)$.

Hence

$$H(p) = \frac{N(p)/Q(p)}{D(p)/Q(p)} \quad (31)$$

We now equate (30) and (31) resulting in

$$Z_{21}^b \cdot Z_{21}^a = N(p) / Q(p) \quad (32a)$$

$$Z_{11}^b - k Z_{22}^a = D(p) / Q(p) \quad (32b)$$

Here after $D(p)/Q(p)$ is split up in rational fractions giving

$$\frac{D(p)}{Q(p)} = k_0 + \frac{k_1}{p} + \sum_{\mu=1}^N \frac{k_\mu}{p + \sigma_\mu} \quad (33)$$

Let the k_μ be numbered in such a way that the first r values of k_μ are positive and the other $N-r$ values are negative. Taking now $k_i = -k_{i-r}$ for $i > r$, we can write (33) as

$$\frac{D(p)}{Q(p)} = \left[k_0 + \frac{k_1}{p} + \sum_{\mu=1}^r \frac{k_\mu}{p + \sigma_\mu} \right] - k \left[\sum_{\mu=1}^{N-r} \frac{k_\mu}{p + \sigma_{\mu+r}} \right] = \frac{D_1(p)}{Q_1(p)} - k \frac{D_2(p)}{Q_2(p)} \quad (34)$$

From (34) we see that $\frac{D_1(p)}{Q_1(p)}$ and $\frac{D_2(p)}{Q_2(p)}$ are realizable RC impedances because all k and l are positive. Therefore we can equate (34) and (32b) giving

$$\left. \begin{aligned} z_{11}^b &= \frac{D_1(p)}{Q_1(p)} \\ z_{22}^a &= \frac{D_2(p)}{Q_2(p)} \end{aligned} \right\} \quad (35)$$

Furthermore (32a) can be written as

$$\frac{N(p)}{Q(p)} = \frac{N_1(p)}{Q_1(p)} \cdot \frac{N_2(p)}{Q_2(p)},$$

leading to

$$\left. \begin{aligned} z_{21}^b &= \frac{N_1(p)}{Q_1(p)} \\ z_{21}^a &= \frac{N_2(p)}{Q_2(p)} \end{aligned} \right\} \quad (36)$$

Equations (35) and (36) lead to realizable RC networks, however as ideal transformers must be excluded the Fialkow-Gerst conditions state that the coefficients of the polynomials $N_1(p)$ and $N_2(p)$ must be positive and smaller than or equal to the corresponding coefficients of $D_1(p)$ resp. $D_2(p)$. This can be arranged by multiplying the numerator and denominator of $H(p)$ with the same proper polynomial and scaling with a certain factor before the synthesis procedure is carried out.

As an example consider the following transferfunction to be realized:

$$H(p) = \frac{V_2}{I_0} = \frac{p}{p^2 + p + 1} = \frac{N(p)}{D(p)}$$

Choosing $Q(p) = p(p+1)$ we find

$$\frac{D(p)}{Q(p)} = 1 + \frac{1}{p} - \frac{1}{p+1} = \frac{p+1}{p} - \frac{1}{p+1}$$

We take $Z_{11}^b = \frac{p+1}{p}$ and $Z_{22}^a = \frac{1}{p+1}$ (i.e. $k=1$)

Furthermore $\frac{N(p)}{Q(p)}$ can be split up in

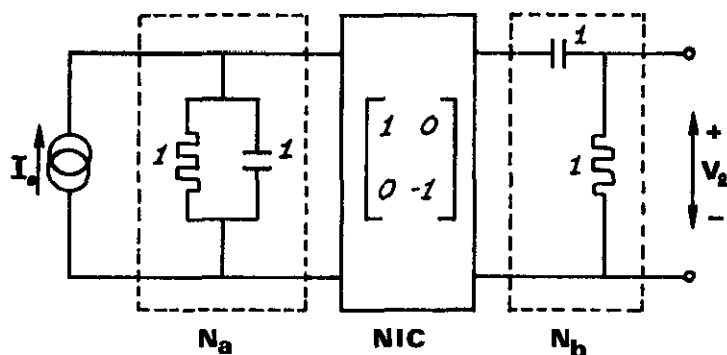
$$\frac{N(p)}{Q(p)} = \frac{p}{p(p+1)} = \frac{p}{p} \cdot \frac{1}{p+1}$$

Hence we may identify $Z_{21}^b = \frac{p}{p} = 1$

$$Z_{21}^a = \frac{1}{p+1}$$

This leads to the realization as given in fig. 37.

The current source with parallel resistor can be changed in a voltage source with series resistor, giving a circuit with voltage transferfunction $H(p)$.



All resistors in Ohms, capacitors in Farads.

fig. 37.

4.1.1 Sensitivity considerations for the Linvill synthesis.

From (30) we find the poles of the transferfunction to be determined by $Z_{11}^b - k Z_{22}^a = 0$. With (35) this becomes

$$\frac{D_1(p)}{Q_1(p)} - k \frac{D_2(p)}{Q_2(p)} = 0$$

Therefore the poles follow from

$$D_1(p) Q_2(p) - k D_2(p) Q_1(p) = 0 \quad (37)$$

Defining the polynomials $A(p) = D_1(p) Q_2(p) = \sum_{m=0}^N a_m p^m$
 and $B(p) = D_2(p) Q_1(p) = \sum_{m=0}^N b_m p^m$

we find (37) to become

$$A(p) - k B(p) = \sum_{m=0}^N (a_m - k b_m) p^m = \sum_{m=0}^N c_m p^m = 0. \quad (38)$$

From (38) the coefficient sensitivity can be calculated as

$$S_k^{c_n} = \frac{k}{c_n} \frac{\partial c_n}{\partial k} = - \frac{k b_n}{c_n}.$$

Especially when a certain small c_n is obtained by subtracting large values for a_n and $k b_n$, the resulting sensitivity $S_k^{c_n}$ can become very large. If the poles of the transferfunction to be realized are situated close to the $j\omega$ - axis, a small change of one of the coefficients of the denominator polynomial may result in right half plane poles and therefore the NIC synthesis may lead to a circuit balancing on the edge of instability.

There is however a degree of freedom in the choice of the polynomial $Q(p)$ and one may expect that this polynomial can be taken in such a way that the pole sensitivity with respect to k can be minimised.

Indeed, for even degree $D(p)$, Horowitz [9] has given the conditions for the polynomial $Q(p)$ as to minimise the pole-sensitivity for variation in the NIC k factor.

The denominator polynomial of $H(p)$ must be split up into

$$D(p) = \prod_{i=1}^{N/2} (p+ai)^2 - 2b_0 p \prod_{i=1}^{N/2-1} (p+bi)^2 \quad \text{with } b_0 > 0; a_i, b_i \geq 0.$$

The polynomial $Q(p)$ then becomes

$$Q(p) = p \prod_{i=1}^{N/2} (p+ai) \prod_{i=1}^{N/2-1} (p+bi).$$

This procedure appears to be quite general as it can be applied in any case in which the difference of two polynomials is involved where in one polynomial can vary with a constant factor.

Calahan [10] has given a method to obtain $Q(p)$ in another way in which no such inhomogeneous system of equations is involved as with the Horowitz method.

In spite of this optimization procedure the Linvill synthesis is only applicable for low degree and low Q factor transferfunctions.

It has however given the first start for active filtersynthesis and gives insight in the problems that can be encountered in these synthesis technics.

4.2 Synthesis method of Yaganisawa.

The structure given by Yaganisawa is depicted in fig. 38, and is also applicable to realize ~~any~~ rational transferfunctions with R-C elements and one current inversion NIC.

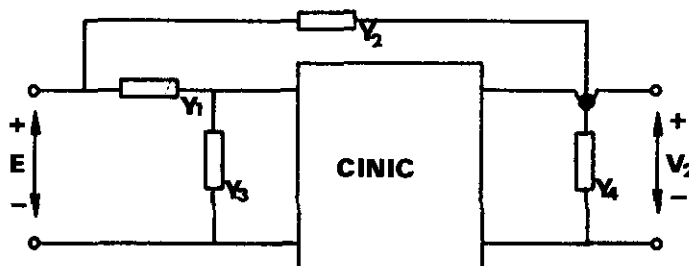


fig. 38.

The transferfunction of this circuit can be calculated as

$$H(p) = \frac{V_2}{E} = \frac{Y_1 - k Y_2}{(Y_1 + Y_3) - k (Y_2 + Y_4)} \quad (39)$$

Following the same procedure as in chapter 4.1 we find

$$H(p) = \frac{\frac{N(p)}{Q(p)}}{\frac{D(p)}{Q(p)}} = \frac{\frac{N(p)}{Q(p)}}{\frac{D(p) - N(p)}{Q(p)} + \frac{N(p)}{Q(p)}} = \frac{(Y_1 - k Y_2)}{(Y_3 - k Y_4) + (Y_1 - k Y_2)}$$

From the above formula we equate

$$\left. \begin{aligned} \frac{D(p)-N(p)}{Q(p)} &= Y_3 - kY_4 \\ \frac{N(p)}{Q(p)} &= Y_1 - k Y_2 \end{aligned} \right\} \quad (40)$$

In the partial fractions expansion of the left hand side of (40) we collect the fractions with positive residues to form Y_1 and Y_3 while the others from Y_2 and Y_4 . For Y_1 etc. to be RC admittances the degree of $Q(p)$ has to be one less than the maximum degree of $N(p)$ or $D(p)$ and again must have its zeros on the negative real axis. Then all admittances can be realized in a Foster parallel RC form and the synthesis is completed.

The sensitivity considerations are generally the same as those of the previous chapter as was shown by J.Schwant [//].

As an example of this synthesis method consider again the realisation of $H(p) = \frac{p}{p^2+p+1}$ with $Q(p) = p+1$.

$$\text{We find } \frac{D(p)-N(p)}{Q(p)} = \frac{p^2+1}{p+1} = p+1 - \frac{2p}{p+1} = Y_3 - k Y_4$$

$$\frac{N(p)}{Q(p)} = \frac{p}{p+1} = Y_1 - k Y_2$$

Taking $k=1$ gives

$$\begin{aligned} Y_1 &= \frac{p}{p+1} & Y_3 &= p+1 \\ Y_2 &= 0 & Y_4 &= \frac{2p}{p+1} \end{aligned}$$

The final filter is given in fig. 39.

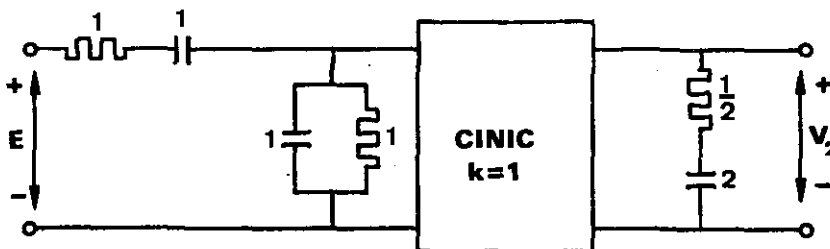


fig. 39.

Recently, Ruprecht [12] has given a synthesis method similar to the Yaganisawa method in which the finite gain of the operational amplifiers as well as the generator output impedance is taken into account.

4.3 Synthesis with the gyrator as a two port [//].

In this method the gyrator is used as a two port element loaded on both ports with RC networks as indicated in fig.40.

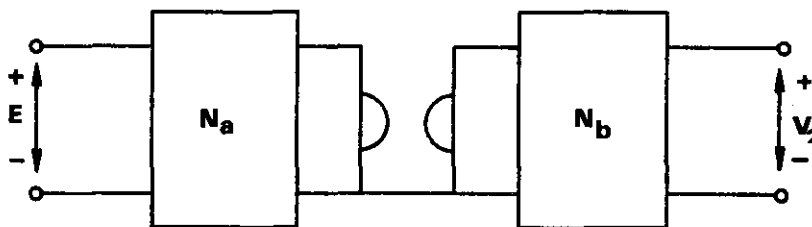


fig. 40.

The transferfunction can be calculated as

$$\frac{V_2}{E} = \frac{-R_g y_{21}^a z_{21}^b}{z_{11}^b + R_g^2 y_{22}^a} \quad (41)$$

Here in R_g is the gyrator resistance of the used gyrator. In order to realize the transferfunction $H(p) = \frac{N(p)}{D(p)}$ with complex poles, it must be split up as follows:

1. Express $D(p)$ as

$$D(p) = \prod_{i=1}^{n/2} (p+a_i)^2 + B_0^2 \prod_{i=1}^{n/2} (p+bi)^2$$

2. Determine $Q(p) = A_0 B_0 \prod_{i=1}^{n/2} (p+a_i) \prod_{i=1}^{n/2} (p+bi)$

3. $H(p)$ follows as

$$H(p) = \frac{N(p)}{Q(p)} \Big/ \frac{D(p)}{Q(p)} \quad \text{with } N(p) = N_1(p) \cdot N_2(p).$$

A comparison between this $H(p)$ and (41) results in

$$\left. \begin{aligned} z_{11}^b &= R_g \frac{\prod_{i=1}^{n/2} (p+a_i)}{A_0 B_0 \prod_{i=1}^{n/2} (p+bi)} & z_{21}^b &= \frac{N_2(p)}{B_0 \prod_{i=1}^{n/2} (p+bi)} \\ y_{22}^a &= \frac{B_0}{R_g A_0} \frac{\prod_{i=1}^{n/2} (p+bi)}{\prod_{i=1}^{n/2} (p+a_i)} & y_{21}^a &= \frac{-N_1(p)}{A_0 \prod_{i=1}^{n/2} (p+a_i)} \end{aligned} \right\} \quad (42)$$

Calahan [13] has shown that the resulting Z_{11}^b and Y_{22}^a will be realizable RC immittances if the following lemma is satisfied.

Lemma: Let the complex poles of $H(p)$ be given by

$$P_{1,2} = R_i e^{j(\pi \pm \varphi_i)} \quad \text{with } 0 < \varphi_i \leq \frac{\pi}{2}; \quad i=1,2,\dots, N/2.$$

Then Y_{22}^a and Z_{11}^b given in (42) are realizable RC immittances if

$$\sum_{i=1}^{N/2} \varphi_i \leq \frac{\pi}{2}.$$

This lemma puts a severe restriction on the realisation of higher-order transferfunctions, however any second and third order transferfunction is realizable as always $\varphi_1 \leq \frac{\pi}{2}$ for stability reasons. Hence this implies that any higher order filter can always be realized with this method by cascading and isolating second or third order sections.

For biquadratic and bicubic low-pass transferfunctions a more direct method can be followed as will be demonstrated below for the bicubic case.

$$\text{Let } H(p) = \frac{1}{kp^3 + lp^2 + mp + 1} = \frac{1}{F(p)}$$

$$\text{From (41) follows } F(p) = - \frac{z_{11}^b + R_g^2 y_{22}^a}{R_g z_{21}^b y_{21}^a}$$

Taking $-z_{21}^b y_{21}^a = \frac{1}{Ap(p+\sigma)}$ results in

$$\frac{1}{R_g} z_{11}^b + R_g y_{22}^a = \frac{F(p)}{Ap(p+\sigma)} = \frac{kp^3 + lp^2 + mp + 1}{Ap(p+\sigma)}$$

Written out in partial fractions this becomes

$$\frac{F(p)}{Ap(p+\sigma)} = k_{\infty} p + \frac{k_1 p}{p+\sigma} + k_2 + \frac{k_3}{p} \quad (43)$$

As will be proven later on we can choose σ so as to produce positive residues in (43).

Splitting up k_2 as $k_2 = k_2^a + k_2^b$ we derive from (43)

$$\frac{1}{Rg} Z_{11}^b = k_2 k_3 + \frac{k_3}{p}$$

$$Rg Y_{22}^a = k_{\infty} p + \frac{k_1 p}{p+\sigma} + k_2^a \tag{44}$$

The partial fraction form in (44) indeed guarantees the realizability for Z_{11}^b and Y_{22}^a .

Furthermore if Z_{11}^b and Y_{22}^a are realized in the Cauer form as depicted in fig. 41, the resulting Y_{21}^a and Z_{21}^b will become

$$Z_{21}^b = \frac{A_1}{p} \quad ; \quad Y_{21}^a = \frac{A_2}{p+\sigma}$$

Hence the transferfunction $H(p)$ is realized except for a constant factor.

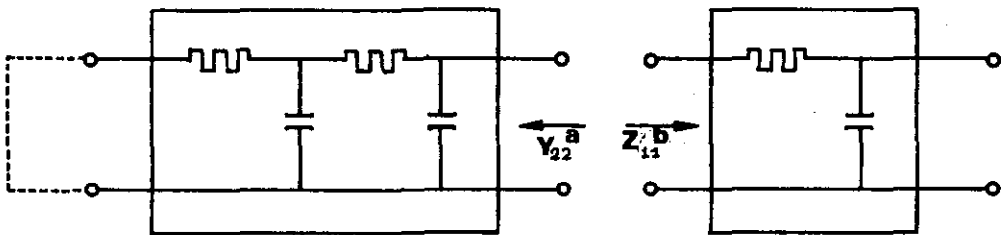


fig. 41.

In order to prove that k_{∞} , k_1 etc. can be made positive we express them in σ and the coefficients of $F(p)$ leading to

$$k_3 = \frac{1}{A\sigma} \quad k_1 = \frac{F(-\sigma)}{A\sigma^2}$$

$$k_2 = \frac{A\sigma-1}{A\sigma^2} \quad k_{\infty} = \frac{K}{A}$$

Requiring all k to be positive then results in

$$\left. \begin{aligned} F(-\sigma) &> 0 \\ A\sigma-1 &> 0 \end{aligned} \right\} \tag{45}$$

Consider next the value $\frac{1}{F(-\frac{1}{A})}$ being

$$F(-\frac{1}{A}) = kp^3 + lp^2 + np + 1 \Big|_{p = -\frac{1}{A}} = -\frac{1}{A^2} \left(\frac{K}{A} - 1 \right)$$

As the Hurwitz condition for $F(p)$ implies $\frac{\sigma}{M} < L$ we have $F(-\frac{1}{M}) > 0$

From the above relation follows that for $\sigma > \frac{1}{M}$ and $\sigma - \frac{1}{M}$ sufficiently small always $F(\sigma) > 0$ can be realized. In this case both relations in (45) are satisfied and therefore all residues k are positive.

This synthesis method will be demonstrated with the following example.

$$\text{Let } H(p) = \frac{1}{p^3 + 3p^2 + 2p + 1}$$

We find $\frac{1}{M} = \frac{1}{2}$ and therefore try $\sigma = 1 > \frac{1}{M}$

This results in $F(\sigma) = 1$, hence (45) is satisfied.

Equation (43) gives with $A=1$

$$\frac{F(p)}{p(p+1)} = \frac{p^3 + 3p^2 + 2p + 1}{p(p+1)} = p + \frac{p}{p+1} + 1 + \frac{1}{p}$$

Taking $R_g = 1$ this results with (44) in

$$z_{11}^a = \frac{1}{p}$$

$$y_{22}^a = p + \frac{p}{p+1} + 1 = \frac{p^2 + 3p + 1}{p+1}$$

The Cauer form for Y_{22}^a is given in fig. 42 and the final filter is depicted in fig. 43.

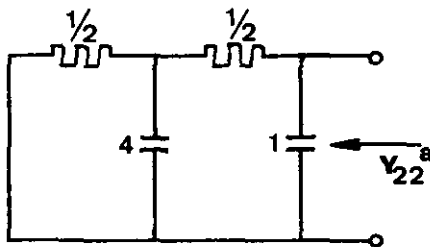


fig. 42.

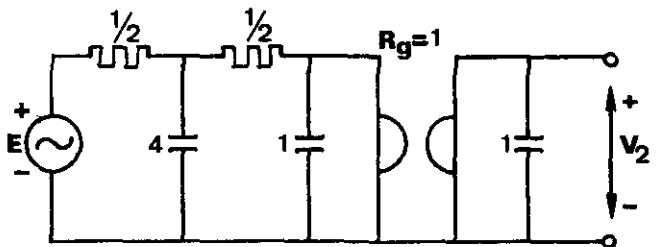


fig. 43.

4.3.1 Sensitivities for the RC gyrator two-port synthesis.

As in this synthesis procedure the poles are determined by a sum of polynomials rather than a difference, the sensitivities are smaller than those of the NIC type realisations and comparable with those of passive filters.

The procedure of chapter 4.3, as proved by Calahan, gives the lowest possible sensitivity with respect to variations in gyrator resistance for every possible decomposition. Furthermore the circuit is always stable for any element value in contrast with the NIC structure.

4.4 Synthesis with PICs by the Antoniou method.

Recently Antoniou [14] has given a synthesis method able to realize every rational transferfunction with PICs and inverting amplifiers. The main advantage of this synthesis method lies in the simplicity of the realization and calculation of the element values.

In realising a voltage transferfunction $H(p)$, Antoniou proceeds as follows:

$$\text{Let } H(p) = \frac{a_0 + a_1 p + \dots + a_n p^n}{b_0 + b_1 p + \dots + b_m p^m} \quad \text{with } 0 \leq |a_i| \leq b_i; \quad b_i > 0. \quad (46)$$

Consider furthermore the voltage transferfunction of a parallel connection of two networks N_a and N_b , given by

$$\frac{V}{E} = \frac{-y_{21}}{y_{22}} = \frac{(-y_{21}^a) + (-y_{21}^b)}{(y_{22}^a) + (y_{22}^b)}. \quad (47)$$

Then (47) implies that $H(p)$ in (46) can be formally realized by the parallel connection of N_a and N_b with

$$\left. \begin{aligned} Y_{21}^a &= a_0 + a_1 p \\ Y_{22}^a &= b_0 + b_1 p \end{aligned} \right\} \quad (48a)$$

$$\text{and } \left. \begin{aligned} -Y_{21}^b &= k_1 p^2 \left(\frac{a_2}{k_1} + \dots + \frac{a_n}{k_1} p^{n-2} \right) \\ Y_{22}^b &= k_1 p^2 \left(\frac{b_2}{k_1} + \dots + \frac{b_m}{k_1} p^{m-2} \right) \end{aligned} \right\} \quad (48b)$$

The network N_a corresponding to (48a) is realized as depicted in fig. 44 in which a switch is positioned to the node labeled "-" if the a_1 corresponding to the connected element is negative or to the node labeled "+" if the concerned a_1 is positive.

The network N_b with Y-parameters given in (48b) is realized by a network N_c in cascade with a PIC with current transfer ratio $1:k_1 p^2$ as depicted in fig. 45.

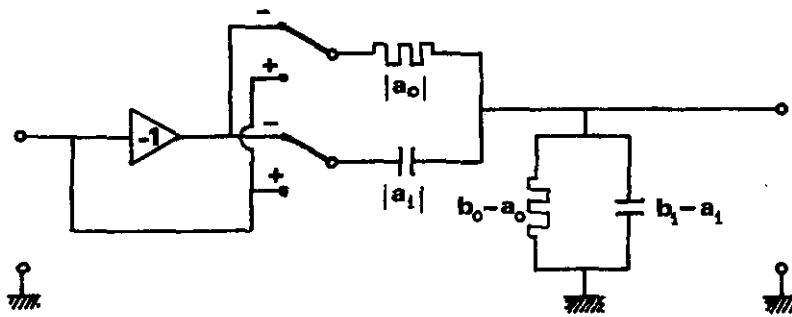


fig. 44.

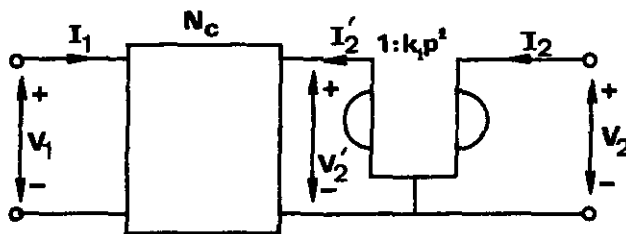


fig. 45.

For N_c holds

$$\left. \begin{aligned} I_1 &= y_{11}^c V_1 + y_{12}^c V_2' \\ I_2' &= y_{21}^c V_1 + y_{22}^c V_2' \end{aligned} \right\} \quad (49)$$

The PIC gives

$$\left. \begin{aligned} V_2 &= V_2' \\ I_2 &= k_1 p^2 I_2' \end{aligned} \right\} \quad (50)$$

From (49) and (50) we find for the network N_b

$$\begin{aligned} I_1 &= y_{11}^c V_1 + y_{12}^c V_2 \\ I_2 &= k_1 p^2 y_{21}^c V_1 + k_1 p^2 y_{22}^c V_2 \end{aligned} ,$$

resulting in

$$\begin{aligned} y_{21}^b &= k_1 p^2 y_{21}^c \\ y_{22}^b &= k_1 p^2 y_{22}^c \end{aligned}$$

Together with (48b) this gives

$$\left. \begin{aligned} -y_{n1}^c &= \frac{a_2}{k_1} + \frac{a_3}{k_1} p + \dots + \frac{a_m}{k_1} p^{m-2} \\ y_{n2}^c &= \frac{b_2}{k_1} + \frac{b_3}{k_1} p + \dots + \frac{b_m}{k_1} p^{m-2} \end{aligned} \right\} \quad (51)$$

Being arrived at this stage we can repeat the whole procedure starting with equations (51), at each step reducing the degree of $H(p)$ with two until all coefficients are realized.

Because of the nature of the above synthesis all denominator coefficients are realized as a sum of maximally two element values. This implies low coefficient sensitivity as to the composing element values and zero coefficient sensitivity for all non composing elements. However the same remarks apply as given in section 3 concerning the possibility that slight changes in the element values may cause instability if high-Q poles are realized.

4.4.1 Special cases for the Antoniou method.

If second or fourth order low-pass filters are to be designed with all transmission zeros at $p = \infty$, the Antoniou procedure can be modified as to result in a circuit with less capacitors. In this case the denominator polynomial can be split up as follows:

For degree 4 $a_0 p^4 + a_1 p^3 + a_2 p^2 + a_3 p + a_4 = \{ \beta_1 + p(p + \alpha_1) \} [\beta_2 + p(p + \alpha_2)] a_0$

For degree 2 $a_0 p^2 + a_1 p + a_2 = \{ \beta_1 + p(p + \alpha_1) \} a_0$

This leads to the realisation as depicted in fig. 46.

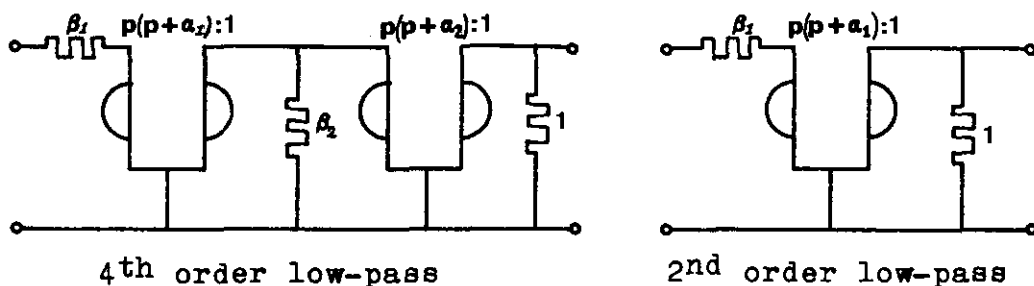


fig. 46.

Furthermore every second order transferfunction may be realized with one PIC with current transfer ratio 1:kp as given in fig. 47, from which the transferfunction can be derived as

$$H(p) = \frac{a_0 p^2 + a_1 p + a_2}{b_0 p^2 + b_1 p + b_2}$$

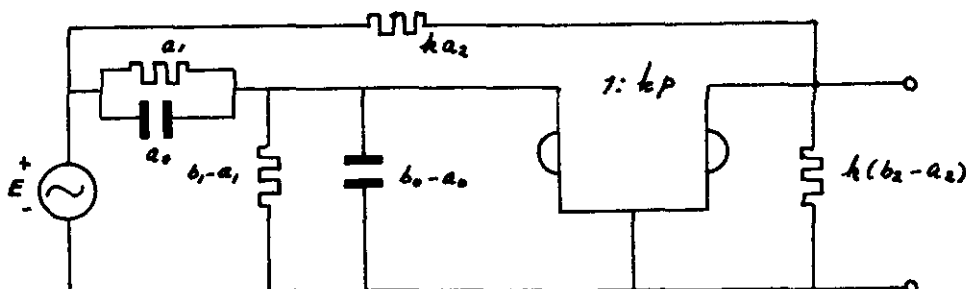


fig. 47.

A negative value for a_1 can be handled in the same way as with the original Antoniou procedure.

As proved by the author [15] the Q factor realized with this circuit is in first approximation independent of the bandwidth of the operational amplifiers in the used PIC circuit of fig 32, and limited to $Q \approx \frac{A_0}{4}$ in which A_0 is the DC open-loop amplifier gain. Therefore this method enables very high Q factors to be realized, insensitive to temperature variations as these mainly cause changes in the amplifier bandwidth.

As the circuit of fig. 47 is also stable for all element values it is very suitable for synthesis by cascading second order sections.

Another interesting feature for this configuration is the possibility to realize second order transferfunctions with zero Q factor sensitivity with respect to changes in the current transfer ratio of the PIC.

Consider for example the circuit of fig. 48 with transferfunction

$$H(p) = \frac{k \frac{R_2}{R_1} p}{p^2 k R_2 C_1 + p \left(k \frac{R_2}{R_1} + k_2 C_2 \right) + 1} \quad (52)$$

The Q factor follows from (52) as

$$Q = \frac{\sqrt{k R_2 C_1}}{k \frac{R_2}{R_1} + R_2 C_2} \quad (53)$$

Equation (53) result in a sensitivity S_k^Q given by

$$S_k^Q = \frac{1}{2} \frac{(R_2 C_2 - k \frac{R_2}{R_1})}{(R_2 C_2 + k \frac{R_2}{R_1})}$$

Taking $k = R_1 C_2$ results in

$$S_k^Q = 0 \quad \text{and} \quad H(p) = \frac{p R_2 C_2}{p^2 R_1 R_2 C_1 C_2 + 2p R_2 C_2 + 1}$$

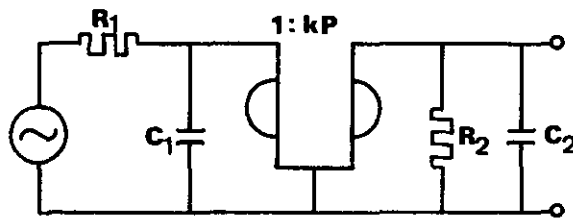


fig. 48.

5. Cascade synthesis with second order sections.

In this section a survey will be given over ~~the~~ various active second order transferfunction realisations which are frequently used in cascade synthesis. Some of these structures can only realize low-pass or high-pass filters, where as other ones are only suitable for low Q-factor transferfunctions. However these circuits use less components as compared with the more general types and may therefore be preferred in some cases.

5.1 Second and third order low-pass Fjälbrant filters.

A. Second order design equations.

Let the transferfunction be given by

$$H(p) = \frac{1}{\alpha p^2 + \beta p + 1}$$

Then the realisation is given in fig. 49 in which the element values are to be determined as follows

1. Choose a value k being the capacitance ratio of C_1 and C_2 .
2. Calculate a , b and c from

$$b = \sqrt{\alpha (1 + 1/k)}$$

$$a = \frac{\alpha}{b}$$

$$c = \frac{a}{k}$$

3. With the values in pnt. 2 the elements become

$$R_1 = 1 \quad C_1 = a$$

$$R_2 = b/c \quad C_2 = c$$

The gain A is determined by

$$A = 2(1 + 1/k) - \beta \frac{\sqrt{1 + 1/k}}{\alpha}$$

The above realisation results in minimum coefficient sensitivity as to variations in amplifier gain given by

$$S_A^A = \frac{2\sqrt{\alpha} \sqrt{(1 + 1/k)}}{\beta} - 1.$$

From this formula it can be seen that k must be taken as large as possible, while small β (i.e. high Q factor) results in high values for S_{β}^A .

Therefore this circuit is only applicable in low Q factor transferfunctions.

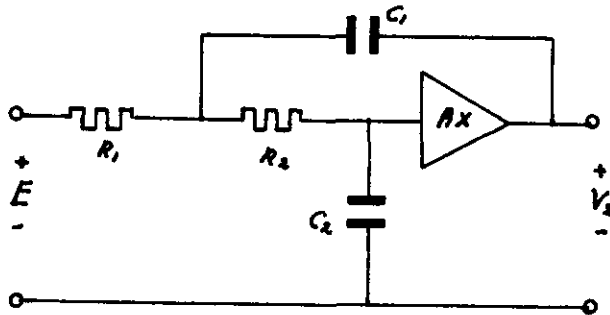


fig. 49.

High-pass filters can be realized by the frequency transformation $p \rightarrow \frac{\omega_0}{p}$. This results in the following impedance transformation:

$$\text{Impedance } R \rightarrow \text{Impedance } \frac{\omega_0 R}{p}$$

$$\text{Impedance } \frac{1}{pC} \rightarrow \text{Impedance } \frac{1}{\omega_0 C}$$

B. Third order design equations

$$\text{Let } H(p) = \frac{1}{Kp^3 + Lp^2 + Mp + 1} = \frac{1}{F(p)}$$

The realization is given in fig. 50 in which the element values are determined as follows:

1. Choose σ_1 with $\sigma_0 < \sigma_1 < \frac{\omega_0}{k}$ in which $-\sigma_0$ is the real pole of $H(p)$. The other two poles are supposed to be complex. Choose σ_2 in such a way that $\sigma_2 > \sigma_1$ and

$$(2 - k\sigma_1)\sigma_2^2 - 11\sigma_2 + 1 > 0.$$

2. Express $\frac{F(p)}{p(p+\sigma_1)(p+\sigma_2)}$ in partial fractions resulting in
$$\frac{F(p)}{p(p+\sigma_1)(p+\sigma_2)} = k_0 + \frac{k_1}{p} + \frac{k_2}{p+\sigma_1} - \frac{k_2}{p+\sigma_2}.$$

3. The element values then follow as

$$R_1 = \frac{k_1}{k_0(k_0 + k_1)} \quad C_1 = \frac{(k_0 + k_1)^2}{\sigma_1 k_1}$$

$$R_2 = \frac{1}{k_0 + k_1} \quad C_2 = k_\infty$$

$$R_3 = \frac{1}{\sigma_2 k_\infty - k_2} \quad C_3 = k_\infty - \frac{k_2}{\sigma_2}$$

The above procedure can be proved to result in positive element values. In order to achieve minimum coefficient sensitivity the values of σ_1 and σ_2 must be taken as small as possible.

For high-pass filters the same considerations hold as in sub A. Again as a consequence of the relative large sensitivities this filter type is only suitable for low Q-factor realizations.

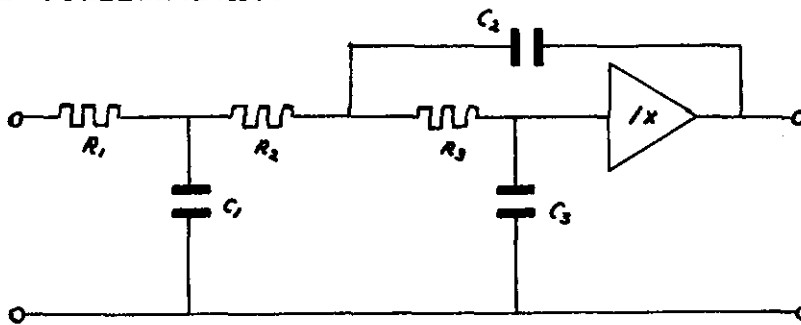


fig. 50.

5.2 Active realizations of second order notch filters with a modified Twin-T network.

In these structures a Twin-T filter is used to produce transmission zeros on the $j\omega$ -axis. Depending on the behaviour of $H(p)$ at $p = 0$ and $p = \infty$ two different structures must be used for the realization, as given in fig. 51.

Together with a frequency transformation the given networks can realize any second degree notch filter. However in order to produce the transmission zeros sufficiently accurate, the element values of the Twin-T must be carefully realized i.e. with tolerances 0.1%.

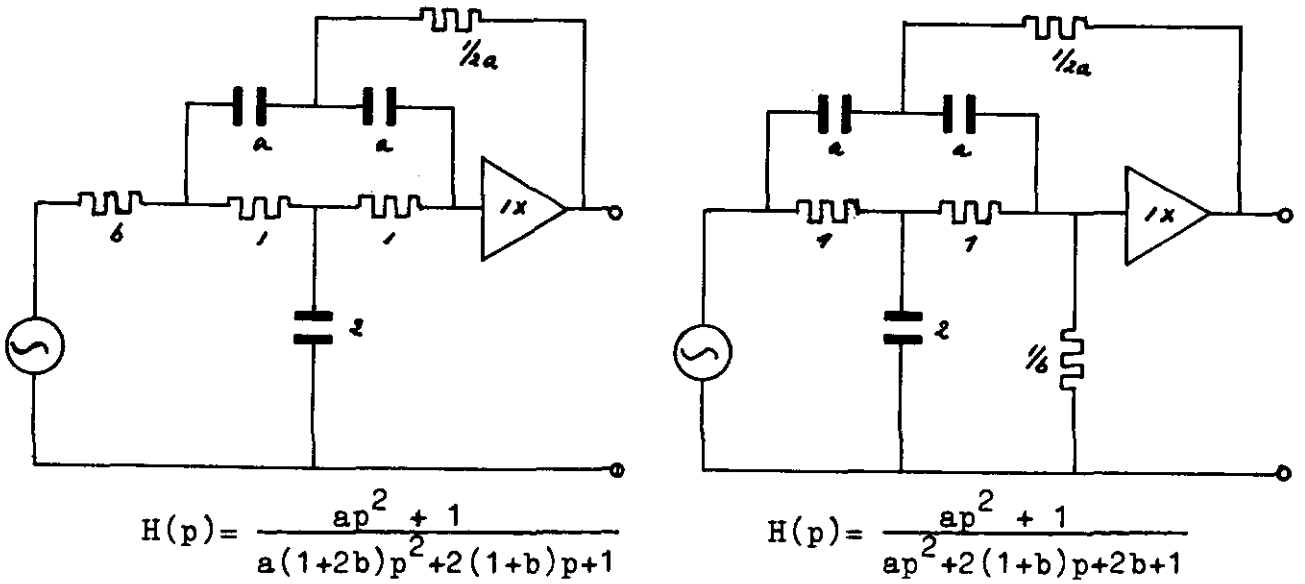


fig. 51.

With these circuits Q factors up to 10 can be achieved for element tolerance of about 1%.

5.3 Active filters employing negative feedback.

Consider the circuit given in fig. 52.

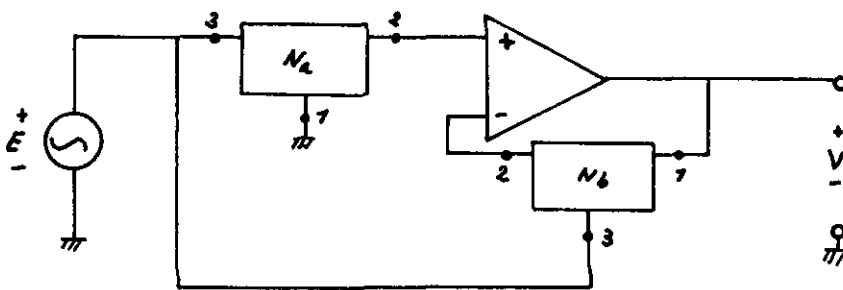


fig. 52.

Supposing the voltage transferfunction of N_a and N_b in the configuration of fig. 53 to be given by H_a and H_b resp. we find the transferfunction of the circuit in fig. 52 to become

$$\frac{V_2}{E} = H(p) = \frac{H_b - H_a}{H_b} \tag{54}$$

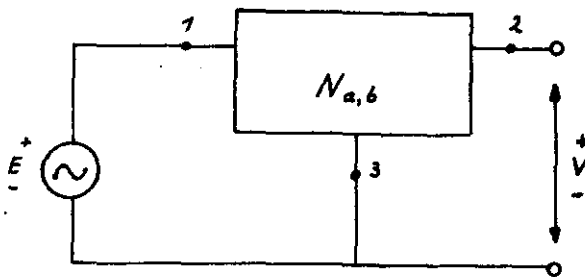


fig. 53.

The poles of $H(p)$ are therefore determined by the zeros of H_b .

As a bridged-T network is able to realize complex zeros we can use this type of network for realizing H_b . Then N_a has to be a suitable network with the same poles as for N_b .

The synthesis proceeds as follows.

Let $H(p)$ be given by $H(p) = k \frac{N(p)}{D(p)}$ in which k is a suitable factor to be determined later on.

Divide numerator and denominator of $H(p)$ by a second degree polynomial $Q(p)$ with its zeros on the negative real axis and all coefficients larger than or equal to the corresponding coefficients of $D(p)$.

This results in

$$H(p) = \frac{k \frac{N(p)}{Q(p)}}{\frac{D(p)}{Q(p)}} \quad (55)$$

Equating numerator and denominator of (54) and (55) gives

$$H_b = \frac{D(p)}{Q(p)} \quad (56a)$$

$$H_a = \frac{D(p) - k N(p)}{Q(p)} \quad (56b)$$

In (56a) we can make a suitable choice for $Q(p)$ so as to produce a simple network for H_b such as the earlier mentioned bridged-T network. Here after we can take k in (56b) small enough to result in a realizable RC network.

At last the transferfunctions in (56a) and (56b) are realized with RC-networks, which networks are then interconnected according to fig. 52.

As an example consider the realization of

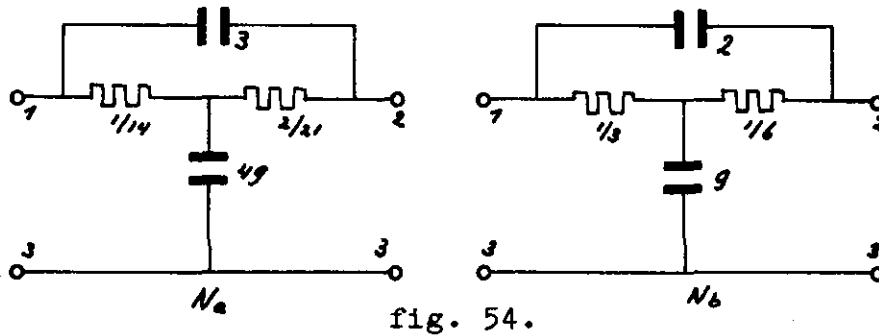
$$H(p) = \frac{kp}{p^2 + p + 1}$$

Taking $Q(p) = p^2 + 4p + 1$ and $k = \frac{1}{2}$ we find

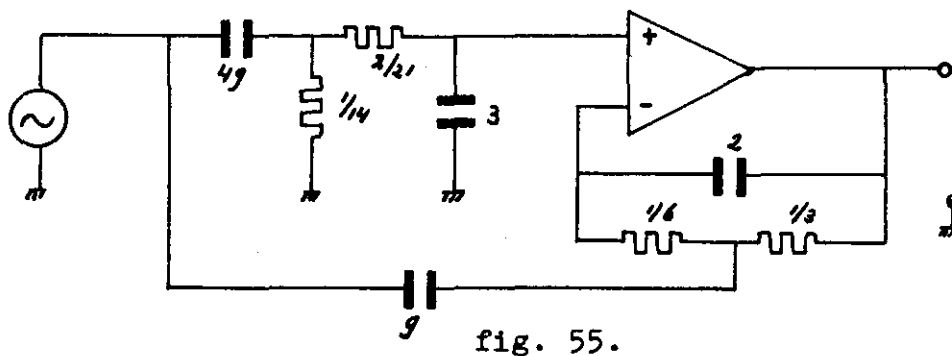
$$H_b = \frac{p^2 + p + 1}{p^2 + 4p + 1}$$

and $H_a = \frac{p^2 + p/2 + 1}{p^2 + 4p + 1}$

The realizations of H_a and H_b are given in fig. 54.



The final network is depicted in fig. 55.



As the poles of the transferfunction are given by the zeros of H_b the sensitivities to element variations are small. Furthermore the polynomial $Q(p)$ can be chosen in such a way as to minimise the pole sensitivity, however this possibility is not further investigated.

5.4 Second order filters with PICs.

As a last example of second order filters we mention the circuit given in chapter 4.4.1 with one PIC having a current transfer ratio of $1:k_p$. As stated there this filter type has a lot of advantages over other realizations for instance its simplicity, stability and the possibility to realize high Q-factors. Together with the minor influence of the operational amplifier bandwidth and the available sensitivity compensation for variations in the PIC current transfer ratio, this circuit will probably be the most suitable for second degree transferfunction realization.

A P P E N D I X

General formulas for the elliptic approximation.

Before deriving these formulas we consider again the Chebychev approximation that can be written in another way as

$$\left. \begin{aligned} \mathcal{D}(u) &= \cos(mu) \\ \Omega &= \cos u \end{aligned} \right\} n = 1, 2, \dots \quad (1)$$

From these formulas one can see that the range $0 \leq \Omega \leq 1$ corresponds to $\frac{\pi}{2} \leq u \leq 0$, overlooking the periodicity in u .

In the given range for u the function $\mathcal{D}(u)$ will pass through n quarter periods varying between +1 and -1. Hence $\mathcal{D}(\Omega)$ will have equiripple behaviour in the passband $0 \leq \Omega \leq 1$ due to the periodicity of $\cos(mu)$.

In transition and stopband however we have $\Omega > 1$ leading to complex u . As $\cos(mu)$ is not periodic for complex values of its argument, the function $\mathcal{D}(u)$ won't be periodic either and therefore cannot have an equiripple stopband behaviour. Because we are interested in equiripple in the passband as well as in the stopband, we will have to construct a transformation comparable with (1) having double periodic properties which are known as elliptic functions.

These functions are defined by means of elliptic integrals as indicated below.

Let $E(x, k)$ be the value of the incomplete elliptic integral of the first kind with argument x and modulus k given by

$$E(x, k) = \int_0^x \frac{dt}{\sqrt{(1-t^2)(1-k^2t^2)}} \quad (2)$$

Furthermore the complete elliptic integral of the first kind denoted by $K(k)$ is defined by

$$K(k) = E(1, k) = \int_0^1 \frac{dt}{\sqrt{(1-t^2)(1-k^2t^2)}} \quad (3)$$

If no confusion can arise $K(k)$ is shortly written as K . The complementary complete elliptic integral of the first kind is defined by

$$K' = E(1, k') = \int_0^1 \frac{dt}{\sqrt{(1-t^2)(1-k'^2t^2)}} \quad (4)$$

with $k' = \sqrt{1-k^2}$ being called the complementary modulus. From (2) we can formally express the value of x in the value of $u = E(x, k)$ by writing

$$x = \operatorname{sn}(u, k) \quad (5)$$

In this way (5) and the relation $u = E(x, k)$ (6) are defining inverse relations.

Its therefore customary to denote from (4)

$$u = \operatorname{sn}^{-1}(x, k) \quad (7)$$

Comparing (6) and (7) we have

$$u = \operatorname{sn}^{-1}(x, k) = E(x, k) = \int_0^x \frac{dt}{\sqrt{(1-t^2)(1-k^2t^2)}} \quad (8)$$

The function $\operatorname{sn}(u, k)$ defined by (5) and (8) is called the Jacobi elliptic sine function.

This function can be proved to be double-periodic with periods $u = 4K$ and $u = 2jK'$ where K and K' are given by (3) and (4) resulting in

$$\left. \begin{aligned} \operatorname{sn}(u + 4K, k) &= \operatorname{sn}(u, k) \\ \operatorname{sn}(u + 2jK', k) &= \operatorname{sn}(u, k) \end{aligned} \right\} \quad (9)$$

Furthermore we have from (3)

$$K = E(1, k) = \operatorname{sn}^{-1}(1, k)$$

and therefore $\operatorname{sn}(k, k) = 1$ (10)

From (8) we also find

$$\operatorname{sn}'(0, k) = 0 \text{ leading to } \operatorname{sn}(0, k) = 0 \quad (11)$$

If u is augmented by a half period $2K$ or jK' we have

$$\begin{aligned} \operatorname{sn}(u+2k, k) &= -\operatorname{sn}(u, k) \\ \operatorname{sn}(u+jk', k) &= \frac{1}{k \operatorname{sn}(u, k)} \end{aligned} \quad (12)$$

Taking $k=0$ in (8) we get

$$\operatorname{sn}^{-1}(x, 0) = \int_0^x \frac{dt}{\sqrt{1-t^2}} = \arcsin(x) = \sin^{-1}(x)$$

resulting in $\operatorname{sn}(x, 0) = \sin(x)$ (13)

Relation (13) clearly shows the periodicity of $\operatorname{sn}(x, k)$ for the special case $k=0$.

The other Jacobi elliptic functions are defined by

$$\begin{aligned} \operatorname{cn}(u, k) &= \sqrt{1 - \operatorname{sn}^2(u, k)} \\ \operatorname{dn}(u, k) &= \sqrt{1 - k^2 \operatorname{sn}^2(u, k)} \end{aligned}$$

and in general if p, q, r are any three of the letters s, c, d, n

$$pq(u, k) = \frac{pr(u, k)}{qr(u, k)} \quad \text{provided that when two letters}$$

are the same the corresponding function is equal to 1.

Thus $\operatorname{ns}(u, k) = \frac{1}{\operatorname{sn}(u, k)}$

From (9), (11) and (12) we find

$$\operatorname{sn}(s \cdot 2k, k) = 0 \quad \text{for } s = \pm 0, 1, 2, \dots$$

and $\operatorname{sn}(jk' + s \cdot 2jk', k) = \operatorname{sn}(jk', k) = \frac{1}{k \operatorname{sn}(0, k)} = \infty$

leading to the pole zero pattern of $\operatorname{sn}(u, k)$ as given in fig. 1.

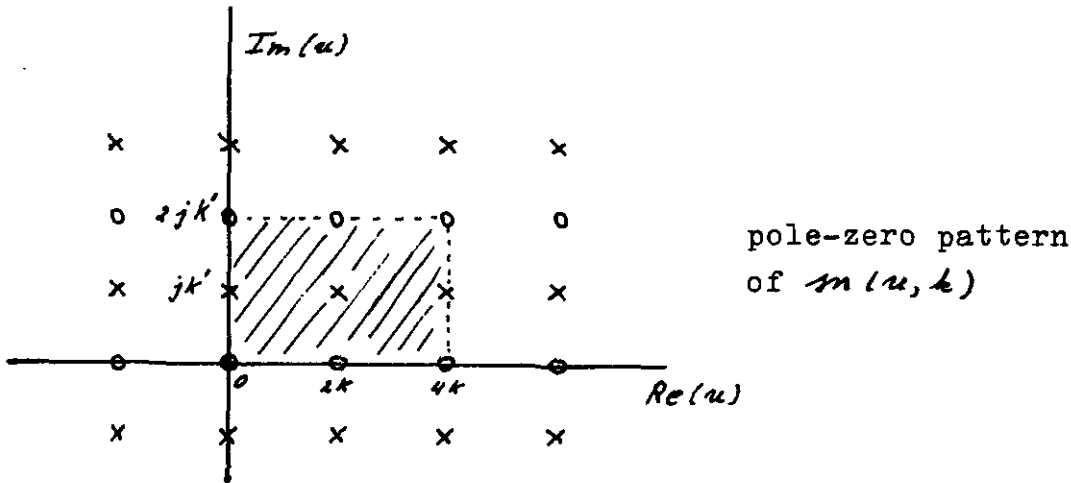


fig. 1.

In this figure the shaded part is repeated periodically through the u -plane.

Derivation of the characteristic function.

In the elliptic approximation we use in comparison with (1)

$$\Omega = \sqrt{k} \operatorname{sn}(u, k) \quad (14)$$

As $\operatorname{sn}(u, k)$ in (14) is double-periodic in u , we may expect that it will be possible to choose $\mathcal{Q}(\Omega)$ in such a way that both pass- and stopband will have equiripple behaviour. In order to find this relation we will examine closer equation (14).

This equation transforms the positive real Ω -axis in the edges of a rectangle in the u -plane by the following way. The range $0 \leq \Omega \leq \sqrt{k}$ leads with (14) to $0 \leq \operatorname{sn}(u, k) \leq 1$, or $0 \leq u \leq k$

Hence $0 \leq \Omega \leq \sqrt{k}$ is mapped on $0 \leq u \leq k$ in the u -plane.

The range $\sqrt{k} \leq \Omega \leq \frac{1}{\sqrt{k}}$ leads to $1 \leq \operatorname{sn}(u, k) \leq \frac{1}{k}$ (15)

From (12) we have $\operatorname{sn}(v + jk', k) = \frac{1}{k \operatorname{sn}(v, k)}$

Taking $v = k$ gives $\operatorname{sn}(k + jk', k) = \operatorname{sn}(k, k) = 1$, hence

$$\operatorname{sn}(k + jk', k) = \frac{1}{k}$$

This leads together with (15) to $\kappa \leq u \leq \kappa + j\kappa'$
 Therefore $\sqrt{\kappa} \leq \Omega \leq \frac{1}{\sqrt{\kappa}}$ is mapped on $\kappa \leq u \leq \kappa + j\kappa'$ in
 the u -plane.

The range $\frac{1}{\sqrt{\kappa}} \leq \Omega \leq \infty$ leads to

$$\frac{1}{\kappa} \leq \operatorname{Im}(u, \kappa) \leq \infty \tag{16}$$

Again from (12) we have

$$\operatorname{Im}(\nu + j\kappa', \kappa) = \frac{1}{\kappa \operatorname{Im}(\nu, \kappa)} \tag{17}$$

From this follows $\sqrt{\kappa} \operatorname{Im}(\nu, \kappa) \cdot \sqrt{\kappa} \operatorname{Im}(\nu + j\kappa', \kappa) = 1$, relating
 the variables $\Omega_1 = \sqrt{\kappa} \operatorname{Im}(\nu, \kappa)$ and $\Omega_2 = \sqrt{\kappa} \operatorname{Im}(\nu + j\kappa', \kappa)$ by

$$\Omega_1 \Omega_2 = 1 \tag{18}$$

We already saw that $0 \leq \nu \leq \kappa$ leads to $0 \leq \Omega_1 \leq \sqrt{\kappa}$ with
 Ω_1 lying in the passband. Then from (18) follows that $\Omega_2 =$
 $= \frac{1}{\sqrt{\kappa} \operatorname{Im}(\nu + j\kappa', \kappa)} = \frac{1}{\Omega_1}$, varies as required by
 (16) from $\frac{1}{\sqrt{\kappa}}$ to ∞ for the same interval of ν , leading
 to frequencies lying in the stopband. Hence frequencies
 Ω_1 and Ω_2 mapped on the u -plane vertical above each
 other on the lines $\operatorname{Im}(u) = 0$ and $\operatorname{Im}(u) = \kappa'$ will be
 related by (18).

On account of the above derivations, the upper left-half
 p-plane is mapped on the shaded part of the u -plane as
 shown in fig. 2 and is periodically repeated there.

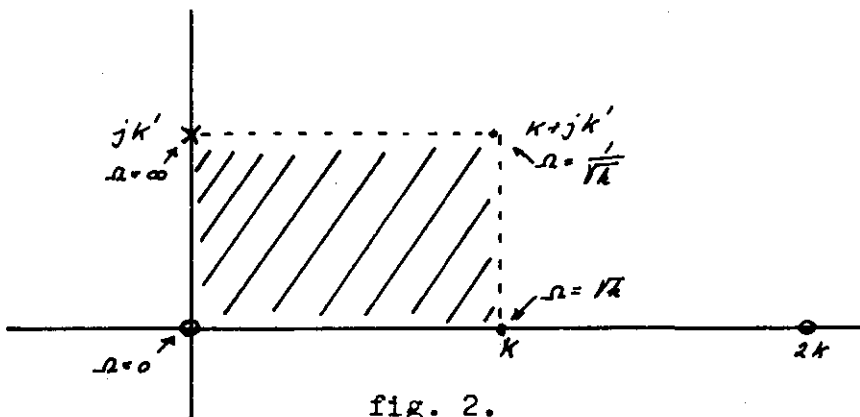


fig. 2.

Next we take

$$\overline{\mathcal{D}}(v) = L \sin(v, L^2) \tag{19}$$

The pole-zero pattern of $\overline{\mathcal{D}}(v)$ is the same as in fig. 1 if the u -plane is changed in the v -plane and k is changed in L^2 ; the periods thus become $4k_2 = 4k(L^2)$, see (3), and $2jk_2' = 2jk(\sqrt{1-L^4})$

As a consequence of (19) along $\text{Im}(v) = 0$ the function $\overline{\mathcal{D}}(v)$ will vary between $+L$ and $-L$ and along $\text{Im}(v) = k_2'$ $\overline{\mathcal{D}}(v)$ varies between $\pm \frac{1}{2}$ and ∞ . Furtheron if we relate u in (14) and v in (19) so that the distance between $u=0$ and $u=k$ equals n times the length k_2 of a quarter period in the v -plane, while at the same time $u=jk'$ coincides with $v=jk_2'$, we can superimpose the corresponding periodic parallelograms of Ω and $\overline{\mathcal{D}}$.

For even n however the point $u=k$ would coincide with $v = s \cdot 2k_2$ ($s = \frac{n}{2}$) hence making $\overline{\mathcal{D}}(v) = 0$ in this point. As the passband edge frequency $\Omega_p = \sqrt{k}$ is mapped to the point $u=k$ this would imply that at this point $\overline{\mathcal{D}}(\Omega)$ would become zero where as the right value has to be $\pm L$. This trouble can be overcome if the whole v -plane is shifted over a distance k_2 in the direction of $-\text{Re}(u)$, before superimposing both planes.

The resulting pole-zero pattern is shown in fig. 3 for $n=3$ and $n=4$.

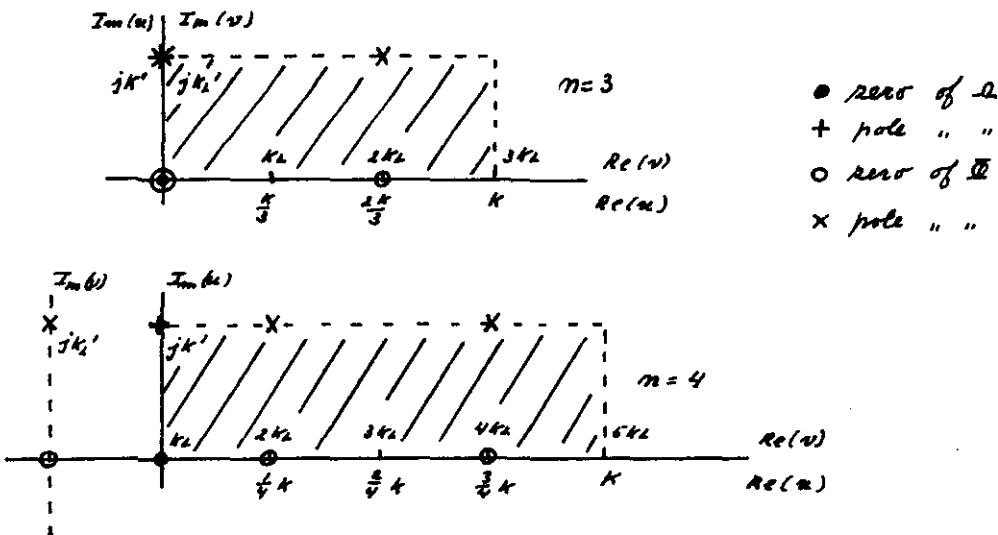


fig. 3.

From fig. 3 we see that

$$\left. \begin{aligned} v &= \left[\frac{m u}{k} + e(m) \right] k_2 \\ \text{with } e(m) &= \begin{cases} 1 & \text{for } m \text{ even} \\ 0 & \text{for } m \text{ odd} \end{cases} \end{aligned} \right\} \quad (20)$$

in order to produce the desired patterns as far as the real u - v -axis is concerned.

As can be seen from fig. 3 also $u = j k'$ must lead to $v = j k_2'$ or $v = k_2 + j k_2'$ for n odd resp. even.

Therefore from (20) follows

$$\begin{aligned} j k_2' + e(m) k_2 &= \frac{j m k'}{k} + e(m) k_2 && \text{giving} \\ \frac{k_2'}{k_2} &= m \frac{k'}{k} && (21) \end{aligned}$$

Relation (21) is an important one in the design-procedure because it relates the three basic design parameters L , k and n in such a way that any two of them prescribe the third.

The desired zeros of $\mathcal{D}(\Omega)$ now follow from (19) by

$$\mathcal{D}(v) = 0 \quad \text{resulting in } v = s \cdot 2 k_2 \quad \text{with } s = \begin{cases} 0, 1, \dots, \frac{m-1}{2} & \text{for } m \text{ odd} \\ 1, 2, \dots, \frac{m}{2} & \text{for } m \text{ even} \end{cases}$$

$$\text{Then (20) gives } u = \frac{k}{m} [2s - e(m)]$$

Finally (14) results in

$$\left. \begin{aligned} \Omega_{0s} &= \sqrt{k} \operatorname{sn} \left[\frac{k}{m} [2s - e(m)], k \right] \\ \text{with } s &= \begin{cases} 0, 1, 2, \dots, \frac{m-1}{2} & \text{for } m \text{ odd} \\ 1, 2, \dots, \frac{m}{2} & \text{for } m \text{ even} \end{cases} \end{aligned} \right\} \quad (22)$$

With (22) we can construct the characteristic function as

$$\mathcal{D}(\Omega) = \Omega^{o(m)} \prod_s \frac{\Omega^2 - \Omega_{0s}^2}{\Omega^2 \Omega_{0s}^2 - 1}$$

$$\text{with } o(m) = \begin{cases} 1 & \text{for } m \text{ odd} \\ 0 & \text{for } m \text{ even} \end{cases}$$

and Ω_{0s} given by (22).

— 0 —

REFERENCES .

- [1] J.K. Skwirzynski : "Design Theory and Data for Electrical Filters",
D.Van Nostrand Co.Ltd., London, 1965.
- [2] Abramowitz & Stegun: "Handbook of Mathematical Functions",
Dover Publ. Inc., New York, 1965.
- [3] T. Fjällbrant: "Canonical Active RC Filters with a Low Transfer Function
Sensitivity", Ericsson Techn., 23, 1967, pp.211-238.
- [4] H.J. Orchard : " Inductorless filters ", Electronics Letters, 2 ,
1966, pp. 224 - 225 .
- [5] H.J. Orchard : " New gyrator circuits obtained by using nullors " ,
Electronics Letters, 4 , 1968, pp. 87 - 88 .
- [6] R.H.S. Riordan : " Simulated inductors using differential amplifiers ",
Electronics Letters, 3 , 1967, pp. 48 - 51 .
- [7] A.W.Keen,J.L.Glover
and R.J. Harris : " Realisation of the circulator concept using
differential - input operational amplifiers " ,
Electronics Letters, 4 , 1968, pp. 389 - 391 .
- [8] L.T. Bruton : " Network Transfer Functions using the concept of
frequency-dependent negative resistance " , IEEE Trans.
on Circuit Theory, CT-16, 1969, pp. 406 - 408 .
- [9] I.M. Horowitz : " Optimization of Negative Impedance Conversion
Methods of Active RC Synthesis " , IEEE Trans. on
Circuit Theory, CT-6 , 1959, pp. 296 - 303 .
- [10] D.A. Calahan : " Notes on the Horowitz optimization procedure", IRE Trans.
on Circuit Theory, CT-7, 1960, pp. 352 - 354 .
- [11] J. Schwant : " Beiträge zur Synthese activer RC-Netzwerke " , Ph.D.
Thesis, University of Stuttgart, Germany, 1969.
- [12] W. Rupprecht: " Synthese activer RC-Netzwerke unter Verwendung eines
Differenzverstärker", A.E.Ü., 23, 1969, pp. 445 - 448 .
- [13] D.A. Calahan: " Sensitivity Minimization in active RC synthesis " , IRE
Trans. on Circuit Theory, CT-9, 1962, pp. 38 - 42 .
- [14] A.Antoniou: "Novel RC-Active-Network Synthesis using Generalized Immit-
tance Converters", IEEE Trans. Circ. Theory, 17, 1970, pp.212-217.
- [15] W.M.G.van Bokhoven: "High-Q active RC-Networks"; to be published.

EINDHOVEN UNIVERSITY OF TECHNOLOGY
THE NETHERLANDS
DEPARTMENT OF ELECTRICAL ENGINEERING

Reports:

- 1) Dijk, J., Jeuken, M., Maanders, E.J.
AN ANTENNA FOR A SATELLITE COMMUNICATION GROUNDSTATION (Provisional Electrical Design)
TH-report 68-E-01, March 1968. ISBN 90 6144 001 7.
- 2) Veefkind A., Blom J.H. and Rietjens L.H.Th.:
THEORETICAL AND EXPERIMENTAL INVESTIGATION OF A NON-EQUILIBRIUM PLASMA IN A MHD CHANNEL
TH-report 68-E-02, March 1968. Submitted to the Symposium on a Magnetohydrodynamic
Electrical Power Generation, Warsaw, Poland, 24-30 July, 1968. ISBN 90 6144 002 5
- 3) Boom, A.J.W. van den and Melis J.H.A.M.:
A COMPARISON OF SOME PROCESS PARAMETER ESTIMATION SCHEMES
TH-report 68-E-03, September 1968 ISBN 90 6144 003 3
- 4) Eykhoff, P., Ophey P.J.M. Severs J. and Oome J.O.M.:
AN ELECTROLYTIC TANK FOR INSTRUCTIONAL PURPOSES REPRESENTING THE COMPLEX-FREQUENCY PLANF
TH-report 68-E-04, September 1968 ISBN 90 6144 004 1
- 5) Vermij L. and Daalder J.E.:
ENERGY BALANCE OF FUSING SILVER WIRES SURROUNDED BY AIR
TH-report 68-E-05, November 1968. ISBN 90 6144 005 X
- 6) Houben J.W.M.A. and Masee P.:
MHD POWER CONVERSION EMPLOYING LIQUID METALS
TH-report 69-E-06, February 1969. ISBN 90 6144 006 8
- 7) Heuvel, W.M.C. van den and Kersten W.F.J.:
VOLTAGE MEASUREMENT IN CURRENT ZERO INVESTIGATIONS
TH-report 69-E-07, September 1969. ISBN 90 6144 007 6
- 8) Vermij, L.:
SELECTED BIBLIOGRAPHY OF FUSES
TH-report 69-E-08, September 1969. ISBN 90 6144 008 4
- 9) Westenberg, J.Z.:
SOME IDENTIFICATION SCHEMES FOR NON-LINEAR NOISY PROCESSES
TH-report 69-E-09, December 1969. ISBN 90 6144 009 2
- 10) Koop, H.E.M., Dijk, J. and Maanders E.J.:
ON CONICAL HORN ANTENNAS.
TH-report 70-E-10, February 1970. ISBN 90 6144 010 6
- 11) Veefkind, A.:
NON-EQUILIBRIUM PHENOMENA IN A DISC-SHAPED MAGNETOHYDRODYNAMIC GENERATOR
TH-report 70-E-11, March 1970. ISBN 90 6144 011 4
- 12) Jansen, J.K.M. Jeuken, M.E.J. and Lambrechtse, C.W.:
THE SCALAR FEED TH-report 70-E-12, December 1969. ISBN 90 6144 012 2
- 13) Teuling, D.J.A.:
ELECTRONIC IMAGE MOTION COMPENSATION IN A PORTABLE TELEVISION CAMERA
TH-report 70-E-13, 1970. ISBN 90 6144 013 0
- 14) Lorencin, M.:
AUTOMATIC METEOR REFLECTIONS RECORDING EQUIPMENT.
TH-report 70-E-14, November 1970. ISBN 90 6144 014 9
- 15) Smets, A.J.:
THE INSTRUMENTAL VARIABLE METHOD AND RELATED IDENTIFICATION SCHEMES.
TH-report 70-E-15. November 1970. ISBN 90 6144 015 7

EINDHOVEN UNIVERSITY OF TECHNOLOGY
THE NETHERLANDS
DEPARTMENT OF ELECTRICAL ENGINEERING

Reports:

- 16) White, Jr. R.C.:
A SURVEY OF RANDOM METHODS FOR PARAMETER OPTIMATIZATION
TH-report 70-E-16, February 1971. ISBN 90 6144 016 5
- 17) Talmon. J.L.:
APPROXIMATED GAUSS-MARKOV ESTIMATORS AND RELATED SCHEMES
TH-report 71-E-17, February 1971. ISBN 90 6144 017 3
- 18) Kalásek, V.:
MEASUREMENT OF TIME CONSTANTS ON CASCADE D.C. ARC IN NITROGEN
TH-report 71-E-18, February 1971. ISBN 90 6144 018 1
- 19) Hosselet, L.M.L.F.:
OZONBILDUNG MITTELS ELEKTRISCHER ENTLADUNGEN
TH-report 71-E-19, March 1971. ISBN 90 6144 019 X
- 20) Arts, M.G.J.:
ON THE INSTANTANEOUS MEASUREMENT OF BLOODFLOW BY ULTRASONIC MEANS
TH-report 71-E-20, May 1971. ISBN 90 6144 020 3
- 21) Roer, Th.G. van de:
NON-ISO THERMAL ANALYSIS OF CARRIER WAVES IN A SEMICONDUCTOR
TH-report 71-E-21, August 1971. ISBN 90 6144 021 1
- 22) Jeuken, P.J. Huber, C. and Mulders, C.E.:
SENSING INERTIAL ROTATION WITH TUNING FORKS
TH-report 71-E-22, September 1971. ISBN 90 6144 022 X
- 23) Dijk, J. and Maanders E.J.:
APERTURE BLOCKING IN CASSEGRAIN ANTENNA SYSTEMS. A REVIEW
TH-report 71-E-23, September 1971. ISBN 90 6144 023 8 (In preparation)
- 24) Kregting, J. and White, Jr. R.C.:
ADAPTIVE RANDOM SEARCH.
TH-report 71-E-24, October 1971. ISBN 90 6144 024 6 (In preparation)